Global and Planetary Change 66 (2009) 208–224

Contents lists available at ScienceDirect

Global and Planetary Change

journal homepage: www.elsevier.com/locate/gloplacha

Comparison of mid-Pliocene climate predictions produced by the HadAM3 and GCMAM3 General Circulation Models

Alan M. Haywood [a,*], Mark A. Chandler [b], Paul J. Valdes [c], Ulrich Salzmann [d], Daniel J. Lunt [c,d], Harry J. Dowsett [e]

[a] School of Earth and Environment, University of Leeds, Leeds, LS2 9JT, UK
[b] Center for Climate Systems Research, Columbia University, 2880 Broadway, New York, New York 10025 USA
[c] School of Geographical Sciences, University of Bristol, University Road, Bristol, BS8 1SS, UK
[d] Geological Sciences Division, British Antarctic Survey, High Cross, Madingley Road, Cambridge, Cambs, CB3 0ET, UK
[e] Eastern Earth Surface Processes, U.S. Geological Survey, 926A National Center, Reston, VA 20192, USA

ARTICLE INFO

Article history:
Received 4 July 2008
Accepted 21 December 2008
Available online 6 January 2009

Keywords:
Pliocene
GCM
intercomparison
BIOME 4
PMIP
Plio-MIP

ABSTRACT

The mid-Pliocene warm period (ca. 3 to 3.3 million years ago) has become an important interval of time for palaeoclimate modelling exercises, with a large number of studies published during the last decade. However, there has been no attempt to assess the degree of model dependency of the results obtained. Here we present an initial comparison of mid-Pliocene climatologies produced by the Goddard Institute for Space Studies and Hadley Centre for Climate Prediction and Research atmosphere-only General Circulation Models (GCMAM3 and HadAM3). Whilst both models are consistent in the simulation of broad-scale differences in mid-Pliocene surface air temperature and total precipitation rates, significant variation is noted on regional and local scales. There are also significant differences in the model predictions of total cloud cover. A terrestrial data/model comparison, facilitated by the BIOME 4 model and a new data set of Piacenzian Stage land cover [Salzmann, U., Haywood, A.M., Lunt, D.J., Valdes, P.J., Hill, D.J., (2008). A new global biome reconstruction and data model comparison for the Middle Pliocene. Global Ecology and Biogeography 17, 432-447, doi:10.1111/j.1466-8238.2007.00381.x] and combined with the use of Kappa statistics, indicates that HadAM3-based biome predictions provide a closer fit to proxy data in the mid to high-latitudes. However, GCMAM3-based biomes in the tropics provide the closest fit to proxy data.

© 2008 Elsevier B.V. All rights reserved.

1. Introduction

General Circulation Models (GCMs) are now routinely used to simulate and predict Earth's present and future climate (e.g. IPCC, 2007). Although there is broad agreement among the models, there are also significant differences in the details of their predictions (Randall et al., 2007). Numerous palaeoclimate simulations have been conducted for various intervals in Earth History (e.g. Kutzbach and Otto-Bliesner, 1982; Barron and Washington, 1982; Valdes and Sellwood, 1992; Kim and Crowley, 2000; DeConto and Pollard, 2003; Huber and Caballero, 2003; Haywood et al., 2007; Sohl and Chandler, 2007). In part, these studies are being carried out in an effort to determine whether or not GCMs can successfully retrodict climatic conditions significantly different from present-day. Through comparison with geological proxy data, such studies may provide us with more confidence in climate model simulations for the future (Williams et al., 2007 and chapters therein). However, it is the norm in palaeoclimate modelling studies for only a single model to be used, meaning the degree to which the results are model dependent is not addressed.

Exceptions to the norm are the modelling studies carried out as part of the Palaeoclimate Modelling Intercomparison Project (PMIP), which was initiated in order to co-ordinate and encourage the systematic study of GCMs and to assess their ability to simulate large differences of climate that occurred in the past (e.g. Joussaume and Taylor, 1995; Hoar et al., 2004; Zheng et al., 2008). It has also served to encourage the preparation of global reconstructions of palaeoclimates that can be used to evaluate climate models (e.g. Prentice and Webb, 1998). The temporal focus of the studies carried out by PMIP has, until now, been restricted to the Last Glacial Maximum and the mid-Holocene climatic optimum, for which detailed reconstructions of palaeoenvironmental conditions exist in a suitable format for integration with GCMs (see the PMIP2 web site for full details of experimental design for the mid-Holocene and LGM: http://pmip2.lsce.ipsl.fr/). To date there have been no co-ordinated model–model comparisons for any pre-Quaternary period. One reason for this is the lack of detailed and internally consistent data sets of palaeoenvironmental boundary conditions from a pre-Quaternary interval.

* Corresponding author. Tel.: +44 113 343 8657; fax: +44 113 343 6716.
E-mail address: earamh@leeds.ac.uk (A.M. Haywood).

0921-8181/$ – see front matter © 2008 Elsevier B.V. All rights reserved.
doi:10.1016/j.gloplacha.2008.12.014

However, one pre-Quaternary data set is available, from the mid-Pliocene warm period (ca. 3 to 3.3 Ma BP), which has been the focus of a major data synthesis and palaeoclimate modelling effort (e.g. Chandler et al., 1994; Sloan et al., 1996; Dowsett et al., 1996, 1999; Haywood et al., 2000a; Jiang et al., 2005). There are many reasons why the mid-Pliocene has proven to be an important time interval to conduct model simulations. The recent Intergovernmental Panel on Climate Change (IPCC) 4th assessment report states "the mid-Pliocene is the most recent interval of geological time when mean global temperatures were ~2 °C to 3 °C above pre-industrial temperatures for a sustained period. Therefore, the mid-Pliocene represents an accessible example of a world that is similar in many respects to what models estimate could be the Earth of the late 21st century" (Jansen et al., 2007).

The mid-Pliocene is recent enough that the continents and ocean basins had reached their present geographic configuration. Taken together, the average of the warmest times during the mid-Pliocene presents a view of the equilibrium state of a globally warmer world, in which atmospheric CO_2 concentrations (estimated to be between 360 and 400 ppm) were likely higher than pre-industrial values (Jansen et al., 2007).

Previous climate modelling studies have identified numerous differences between the climate states of the mid-Pliocene and present-day (e.g. Chandler et al., 1994; Sloan et al., 1996; Haywood et al., 2000a; Haywood and Valdes, 2004). As well as a 2 °C to 3 °C increase in global mean surface temperatures, the position of the Inter-Tropical Convergence Zone (ITCZ) may have differed (e.g. Chandler et al., 1994). Hadley Circulation may have been affected allowing more precipitation to fall over wider geographical areas of the tropics and sub tropics leading to a significant reduction in the area of low latitude deserts (Haywood et al., 2000a). Monsoon behaviour in Africa and East Asia was potentially dramatically different in terms of the geographical focus of the monsoons and their intensity (Chandler et al., 1994; Sloan et al., 1996; Haywood et al., 2000a). Warmer mid-to-high-latitude sea surface temperatures (SSTs) and reduced sea ice coverage, combined with regional differences in high-latitude low-pressure and sub-tropical high-pressure cells, may have promoted intensification of winter storms in the Northern and Southern Hemispheres (Haywood et al., 2000b). In terms of the relative contribution of different forcing factors to mid-Pliocene warmth, Haywood and Valdes (2004) suggested that altered geographical coverage of cloud cover is nearly as important as altered trace gases or ice-albedo feedbacks and that high-latitude warmth during the mid-Pliocene was promoted by greater cloud cover.

Although intriguing, the results outlined above could be highly model dependent (e.g. cloud cover feedbacks). Haywood et al. (2000a) attempted a model intercomparison between the HadAM3 GCM and versions of the Goddard Institute for Space Studies (GISS) and National Center for Atmospheric Research (NCAR) GCMs which had been used previously to produce mid-Pliocene climatologies. However, this comparison was severely hampered due to the fact that the boundary conditions in each of these studies were not the same. The GISS model study (Chandler et al., 1994) simulated mid-Pliocene climates in the Northern Hemisphere and used an 8°×10° version of the PRISM data set (Pliocene Research Interpretations and Synoptic Mapping) which is referred to as PRISM0. The NCAR GENESIS model study (Sloan et al., 1996) considered the Southern as well as Northern Hemisphere but used the PRISM1 boundary conditions whereas the more recent HadAM3 GCM studies have used the PRISM2 data set (e.g. Haywood et al., 2000a).

This paper presents results from a pilot study which assesses the possible degree of model dependency for mid-Pliocene GCM climatologies. We present a comparison between surface air temperature, precipitation rate and total cloud cover derived from the climate models GCMAM3 and HadAM3. Data/model comparison is facilitated by the use of the BIOME 4 mechanistic model of vegetation (Kaplan, 2001). Our focus on comparing the respective models predictions of surface air temperature, precipitation and cloud cover is justifiable given that the geological proxy climate record for the Pliocene cannot provide information on other climate variables (other than surface temperature and precipitation) to aid in the assessment of model performance. A comparison of total cloud cover is required however, since this, along with monthly mean surface air temperature and precipitation, is needed to run the BIOME 4 model. It is hoped that this work will serve to encourage a larger-scale data-model-to-model comparison for this interval in the future.

2. Methods

2.1. The climate models — HadAM3 and GCMAM3 GCMs

The particulars of the version of the Hadley Centre model used in this study (hereafter referred to as the HadAM3) are well documented (Pope et al., 2000). HadAM3 was developed at the Hadley Centre for Climate Prediction and Research, which is a part of the UK Meteorological Office. The horizontal resolution of the model is 2.5° in latitude by 3.75° in longitude. This gives a grid-spacing at the equator of 278 km in the north–south direction and 417 km in the east–west direction and is approximately comparable to a T42 spectral model resolution. The model has 19 layers in the vertical, a time step of 30 min and includes a radiation scheme that can represent the effects of trace gases (Edwards and Slingo, 1996). A parameterization of simple background aerosol climatology is also included (Cusack et al., 1998). The convection scheme employed is that of Gregory et al. (1997), and a land-surface scheme includes the representation of the freezing and melting of soil moisture. The representation of evaporation includes the dependence of stomatal resistance on temperature, vapour pressure and CO_2 concentration (Cox et al., 1999). The sea ice component uses a relatively simple thermodynamic scheme and contains parameterizations of ice drift and leads (Cattle and Crossley, 1995).

The second atmospheric GCM used is the GISS Global Climate Middle Atmosphere Model version 3 (hereafter referred to as the GCMAM3), which is described in detail by Rind et al. (2007). For our experiments we used a relatively coarse vertical resolution of 23 layers and a top near the base of the mesopause (0.001 mb, ~80 km). As with most GCMs, the model calculates temperature, pressure, winds and specific humidity as prognostic variables, using the conservation equations for mass, energy, momentum and moisture. Unlike other models however, GCMAM3 uses fourth-order differencing schemes in the momentum and mass equations and a quadratic-upstream scheme for heat and moisture advection, which implicitly enhances an absolute model resolution of 4°×5° horizontal gridding to 1.3°×1.6° and the GISS 2.0°×2.5° grid, to 0.7°×0.8° (see Schmidt et al., 2006). The existing radiation physics includes calculations for trace gas constituents (CO_2, CH_4, N_2O, CFCs, and O^3) and aerosols (natural and anthropogenic) and is capable of simulating the effects of large forcing changes in constituents such as volcanic aerosols and greenhouse gases. The forcings are assigned at start-up or can be altered transiently throughout an experiment. In addition, a parameterized gravity-wave drag formulation incorporates gravity-wave momentum fluxes that result from flow over topography, wind shear and convection. The generation, propagation and drag are all a function of the calculated variables at each grid box for the various vertical levels. Results from previous versions of the GISS Middle Atmosphere Model are widely published in major scientific studies (e.g. Balachandran and Rind, 1995; Shindell et al., 2001; Rind et al., 2001a,b, 2005). GCMAM has also been shown to be robust and flexible enough to perform a variety of long integrations with extreme palaeoclimate scenarios (Rind et al., 2001a). See Table 1 for a systematic comparison of GCMAM3 versus HadAM3 dynamics, parameterizations schemes and resolution.

Table 1
Showing dynamical characteristics, parameterizations and resolution for both GCMAM3 and HadAM3.

GCMAM3	HadAM3
Dynamics: Grid point, Arakawa B-grid, hybrid vertical co-ordinates. Quadratic upstream scheme (QUS) for advection 23 levels, model top .001 mb, timestep 7.5 min	*Dynamics*: Hydrostatic, grid point, Arakawa B-grid, hybrid vertical co-ordinates. Eulerian advection scheme 19 model levels, middle of top level 5 mb, timestep 30 min
Clouds: Rind et al. (2007), Del Genio et al. (1996)	*Clouds*: Prognostic (Gregory and Morris, 1996)
Precipitation: Schmidt et al. (2006), Rind et al. (2007)	*Precipitation*: Senior and Mitchell (1993), Gregory (1995)
Convection: Rind et al. (2007), Del Genio et al. (1996)	*Convection*: Moist and dry mass-flux scheme (Gregory and Rowntree, 1990), convective downdrafts (Gregory and Allen, 1991).
Radiation: Schmidt et al. (2006), Oinas et al. (2001), Lacis and Oinas (1991), Hansen et al. (1983)	*Radiation*: Edwards and Slingo (1996), Cusack et al. (1999)
Gravity-wave drag: Rind et al. (2007, 1999, 1988)	*Gravity-wave drag:* Gregory et al. (1998)
Boundary layer scheme: Schmidt et al. (2006), Rind et al. (2007)	*Boundary layer scheme:* Smith (1990)
Horiz. Res: 72×46 (4°×5°) with effective resolution for all tracers at ~1.3°×~1.6° through use of the QUS	*Horiz. Res*: 96×73 (2.5°×3.75°) ~T42

2.2. Boundary conditions and experimental design

Four atmospheric GCM simulations were conducted using the HadAM3 and GCMAM3 GCMs (two experiments per model, one present-day simulation and one mid-Pliocene simulation). For each model an identical mid-Pliocene simulation was performed. For the mid-Pliocene simulations, hereafter referred to as HadAM3^{MP} and GCMAM3^{MP}, trace gas concentrations were set to identical values (e.g. CO_2 = 315-ppmv). The chosen value for atmospheric CO_2 is low given available proxy estimates of mid-Pliocene atmospheric CO_2 concentrations that are available (Raymo and Rau, 1992; Kürschner et al., 1996; Raymo et al., 1996). This value is historical as it was the value used in the first mid-Pliocene climate modelling study using the GISS GCM (Chandler et al., 1994) and Hadley Centre model (Haywood et al., 2000a). For consistency with previous AGCM simulations CO_2 at 315 ppmv is used in this study. However, since results in this study are derived from atmosphere-only GCMs, using prescribed ocean conditions, the given concentration of atmospheric CO_2 is not greatly significant as ocean temperatures are unable to respond to the altered greenhouse concentration (see Table 2 for summary details of model simulations).

The mid-Pliocene has been the subject of intense study by the PRISM Group. The PRISM data set has evolved from a series of studies that summarised conditions at a large number of marine and terrestrial sites and areas (e.g. Cronin and Dowsett, 1990; Poore and Sloan, 1996). The first global reconstruction of mid-Pliocene climate (PRISM1) was based upon sixty-four marine and seventy-four terrestrial sites and included data sets representing annual vegetation and land ice, monthly SST and sea ice, sea level and topography (Dowsett et al., 1996; Thompson and Fleming, 1996). PRISM2 was a revision of PRISM1 incorporating the following significant changes:

(1) Additional marine sites were added to improve coverage. Sites from the Mediterranean and Indian Ocean were incorporated for the first time.
(2) All SST estimates were recalculated using a new core-top calibration based upon the Reynolds and Smith (1995) adjusted optimum interpolation (AOI) data set.
(3) The Pliocene sea level was re-set at +25 m in keeping with isotopic data not available when PRISM1 was released.
(4) PRISM2 used model results to guide the areal and topographic distribution of Antarctic ice. This resulted in a much more realistic Antarctic ice configuration in tune with the 25 m sea level rise.

The PRISM2 data set, summarised in the following paragraphs, is a digital palaeoclimate reconstruction of the Earth based upon analysis of mid-Piacenzian age samples from both the marine and terrestrial realms (Dowsett et al., 1999; Dowsett, 2007a). The reconstruction features increased warming at mid to high-latitudes and relatively unchanged (from present day values) tropical regions. Ocean circulation was similar to present day but the major western boundary currents appear to have transported more heat to higher latitudes. Forests grew at the edge of the Arctic shoreline. The northern hemisphere (Arctic Ocean) was seasonally ice-free and sea ice conditions in the Antarctic were greatly reduced. Continents were in the same basic positions as present day, but the PRISM2 reconstruction showed orographic changes in North America and Africa.

The PRISM2 marine data set uses 77 localities distributed globally, from which SST and sea ice distribution is determined. These estimates are based upon quantitative analyses of planktic foraminifer, diatom, radiolarian and ostracode assemblages. Wherever possible, multiple proxies of temperature were included to confirm estimates.

Northern Hemisphere sea ice distribution for the mid-Piacenzian (mid-Pliocene) is based primarily upon marine submerged and emerged (outcrops) deposits along the margins of the Arctic Basin. Southern Ocean sea ice extent is primarily based upon the distribution of sea ice-related diatoms and the presence of diatomaceous oozes that do not occur today south of the northernmost extent of Southern Hemisphere sea ice. Other evidence for reduced sea ice comes from silicoflagellates and opal sedimentation.

Table 2
Details on model resolution, experiment types with initial conditions and boundary condition details provided.

GCM	Model resolution	Solar constant (W m^{-2})	Eccentricity	Obliquity	Precession	Sea-ice leads fraction (%)
GCMAM3	4°×5°	1365	0.0167	23.44	282.9	5
HadAM3	2.5°×3.75°	1365	0.0167	23.44	282.9	10 (via sea-ice input files)

Simulation name	Integration length (yr)	Averaging period (yr)	Land/sea mask and topography	SSTs	Land and sea-ice	Land cover	CO_2 (ppmv)	CH_4 (ppbv)	N_2O (ppbv)	CFC^{11} (pptv)	CFC^{12} (pptv)
GCMAM3^{PD}	20	12	NASA/GISS from ETOPO5	Rayner et al. (2003)	Land ice: ETOPO5 (NOAA, 1988) Sea-ice: Rayner et al. (2003)	Matthews (1985), Abramopoulos et al. (1988)	315	1200	287	0	0
GCMAM3^{MP}	20	12	PRISM2	PRISM2	PRISM2	PRISM2	315	1250	287	0	0
HadAM3^{PD}	30	10	ETOPO5 (NOAA, 1988)	Reynolds and Smith (1995)	Jasperson et al. (1990)	Wilson and Henderson-Sellers (1985)	346	790	285	222	382
HadAM3^{MP}	20	12	PRISM2	PRISM2	PRISM2	PRISM2	315	1250	287	0	0

Table 3
Annual, DJF and JJA global mean, land mean and ocean mean surface air temperature (°C) and total precipitation rate (mm/day) for mid-Pliocene simulations produced by the GCAM3 and HadAm3 models.

Variable	GCMAM3			HadAM3		
Averaging period	Annual	DJF	JJA	Annual	DJF	JJA
Surface air temperature (in °C) — global mean	15.55	14.11	16.95	16.38	14.59	18.12
Surface air temperature (in °C) — land mean	10.89	6.62	15.26	11.72	5.72	17.80
Surface air temperature (in °C) — ocean mean	17.45	17.16	17.64	18.13	17.91	18.24
Precipitation (in mm/day) — global mean	2.96	2.96	3.01	2.97	2.96	3.01
Precipitation (in mm/day) — land mean	2.50	2.28	2.72	2.42	2.16	2.51
Precipitation (in mm/day) — ocean mean	3.14	3.23	3.12	3.18	3.26	3.20

Pliocene orography was poorly known at the time the PRISM2 reconstruction was published. Even today, our understanding of changes in uplift rates and erosion over the past three million years allows for only a generalised modification of present day orography as a first order estimate for mid-Pliocene conditions. Never-the-less, the PRISM2 reconstruction used palaeobotanical evidence to suggest that the East African rift areas were 500 m higher during the mid-Pliocene relative to today (Dowsett et al., 1999). In contrast, palaeoelevation of the western cordiellera of North America and northern South America was lower relative to present values. Large elevation differences are noted in both Greenland and Antarctica due to significant removal of continental ice from those regions.

PRISM2 land ice distribution and volume was closely associated with stable isotopic and stratigraphic sea level estimates. Antarctic Ice distribution was based upon a stable ice sheet configuration predicted by an ice sheet model (Dowsett et al., 1999).

The PRISM2 vegetation reconstruction was compiled from fossil pollen and plant macrofossil data from over 74 terrestrial sites covering all continents. Whenever practical, pollen was recovered from marine sequences to establish true continental–marine correlations. PRISM2 uses seven land cover categories (desert, tundra, grassland, deciduous forest, coniferous forest, rainforest, and land ice that are a simplification of the 22 land cover types of Matthews (1985).

To produce the HadAM3^{MP} and GCMAM3^{MP} simulations, the GCMs were forced with continental configurations changed by a 25 m sea level rise, reduced ice-sheet size for Greenland (by 50%) and Antarctica (by 33%), altered vegetation distribution, and reconstructed sea surface temperatures from the PRISM2 data set (for further details see Table 2). The models were integrated for present-day and the mid-Pliocene for between 20 and 30 simulated years. Climatological means were calculated from the final 10 years. Analysis of the surface temperature time series for all experiments indicates that the simulations have reached an equilibrium condition. Global, land and ocean mean values for surface air temperature and total precipitation rate are shown in Table 3.

3. GCMAM3 and HadAM3 — mid-Pliocene minus present-day

3.1. Surface air temperature (°C)

We begin by examining the GCMAM3 and HadAM3 GCMs difference in annual and seasonal mean surface air temperatures, between the mid-Pliocene and present-day. Given the use of identical boundary conditions, it is unsurprising, but nonetheless reassuring, to see that both models simulate very similar trends at the global scale. Both models predict a pattern of little or no difference in tropical temperatures. Increased surface air temperatures are evident in the mid- and high-latitudes of both hemispheres (Figs. 1 and 2). The largest increase in surface air temperatures occurs poleward of 60° in both hemispheres. Warmest temperatures over the oceans occur in the Northern Hemisphere, a function of the prescribed SSTs from the PRISM2 data set. Limited areas of cooler temperatures occur in the subtropics and, additionally, across East Africa where mid-Pliocene topographic relief is higher than present day in the PRISM2 data set (Fig. 2).

Both models simulate the largest magnitude of warming in the high-latitudes of the winter hemisphere. During June, July, and August (JJA), both models simulate a belt of decreased surface air temperatures across North Africa, Arabia and into parts of India, although this area of cooling is more geographically extensive in GCMAM3 (Fig. 2).

3.2. Total precipitation rate (mm/day)

The geographical distribution of mid-Pliocene precipitation is broadly similar in both models to the modern (Figs. 1 and 3), though precipitation increases of 2 mm/day are seen in both models in each hemisphere, during both winter and summer (Fig. 3). During winter, precipitation rates over the continents show little difference, though the sign of change over the Andes is opposite in the two GCMs. Over the oceans, major precipitation changes are positively correlated with SST anomalies. Precipitation rates increase over the warm ocean regions (for example, over the northern most extension of the Gulf Stream) but decreases are evident in the tropics although no significant tropical SST differences are seen in PRISM2 input data. These tropical precipitation changes are somewhat more intense in GCMAM3 than in the HadAM3.

During summer the pattern is more complex. Simulated precipitation rates increase substantially throughout the subtropics including extreme intensification over Africa and the Middle East. HadAM3 shows this region of increased precipitation extending across the Atlantic Ocean as well, whereas the GCMAM3 does not. Large decreases are simulated over the eastern Atlantic, over the Bay of Bengal, and over portions of the Indian Ocean. In addition, smaller decreases occur over Central America and North America (Fig. 3).

The models indicate that the southern limit of the Hadley Cell in the mid-Pliocene is in a similar position to the modern. However, the northern limit is displaced further to the North. This results in a net broadening of the Hadley Cell, which allows more precipitation to fall over a larger geographical area. The difference in the position of the modelled mid-Pliocene Hadley Cell is caused by the simulated reduction in the equator-to-pole temperature gradient (see Figs. 1 and 2). Broadening of the Hadley Cell explains a number of responses in the models observed at equatorial and low-latitudes such as the increased precipitation, evaporation and subsequent reduction of surface temperatures (as was reported in Haywood et al., 2000a).

In the extra-tropical storm tracks during winter, precipitation rates tend to decrease across the Eastern U.S. Atlantic Coast but actually increase downstream over the North Atlantic Ocean and the United Kingdom. The effect is particularly pronounced in the HadAM3 and less so in the GCMAM3. The precipitation rate in HadAM3 is similarly more sensitive over Southern Hemisphere winter storm tracks than GCMAM3. Precipitation rates in HadAM3 are decreased over the South Pacific, but increased over the South Atlantic and Indian Oceans.

3.3. Total cloud cover (%)

The character of the cloud distribution simulated by GCMAM3 and HadAM3 suggests a clear trend in the response between mid-Pliocene and present-day conditions. As an annual mean both models predict increased total cloud cover over Greenland and Antarctica of up to 40%. HadAM3 predicts an increase in cloud cover of up to 20% over the Arctic Ocean which is not replicated in GCMAM3. Both models predict a strong increase (5 to 45%) in cloud cover over North Africa associated with the model predictions of enhanced total precipitation rates in

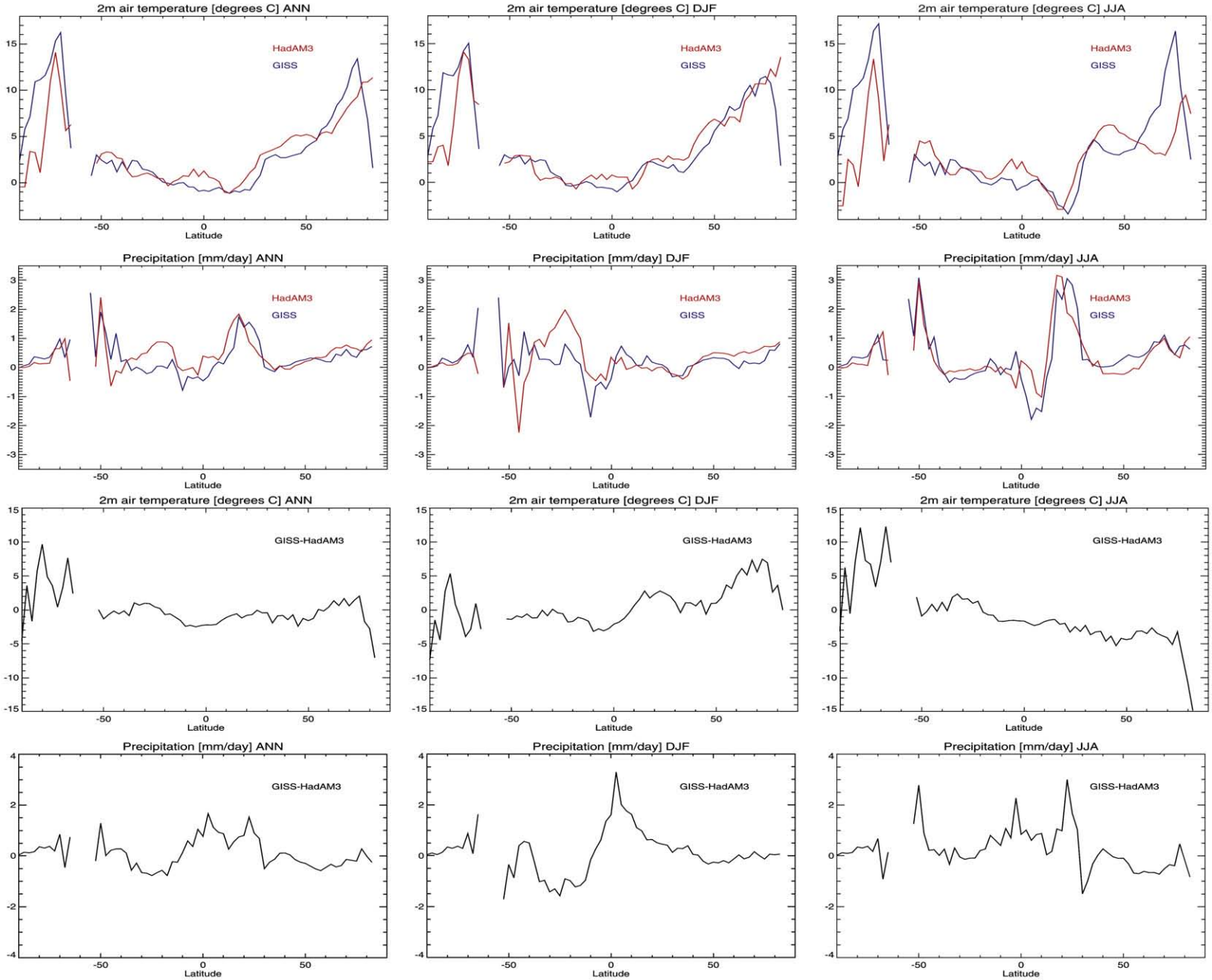

Fig. 1. Annual, December, January and February (DJF) and June, July and August (JJA) mean difference (mid-Pliocene minus present-day) in surface air temperature (°C) and total precipitation rate (mm/day) averaged over land, and as a function of latitude, predicted by the GCMAM3 and HadAM3 climate models. Differences between GCMAM3 and HadAM3 mid-Pliocene annual, DJF and JJA mean surface air temperature and total precipitation rate averaged over land, and as a function of latitude, are also shown.

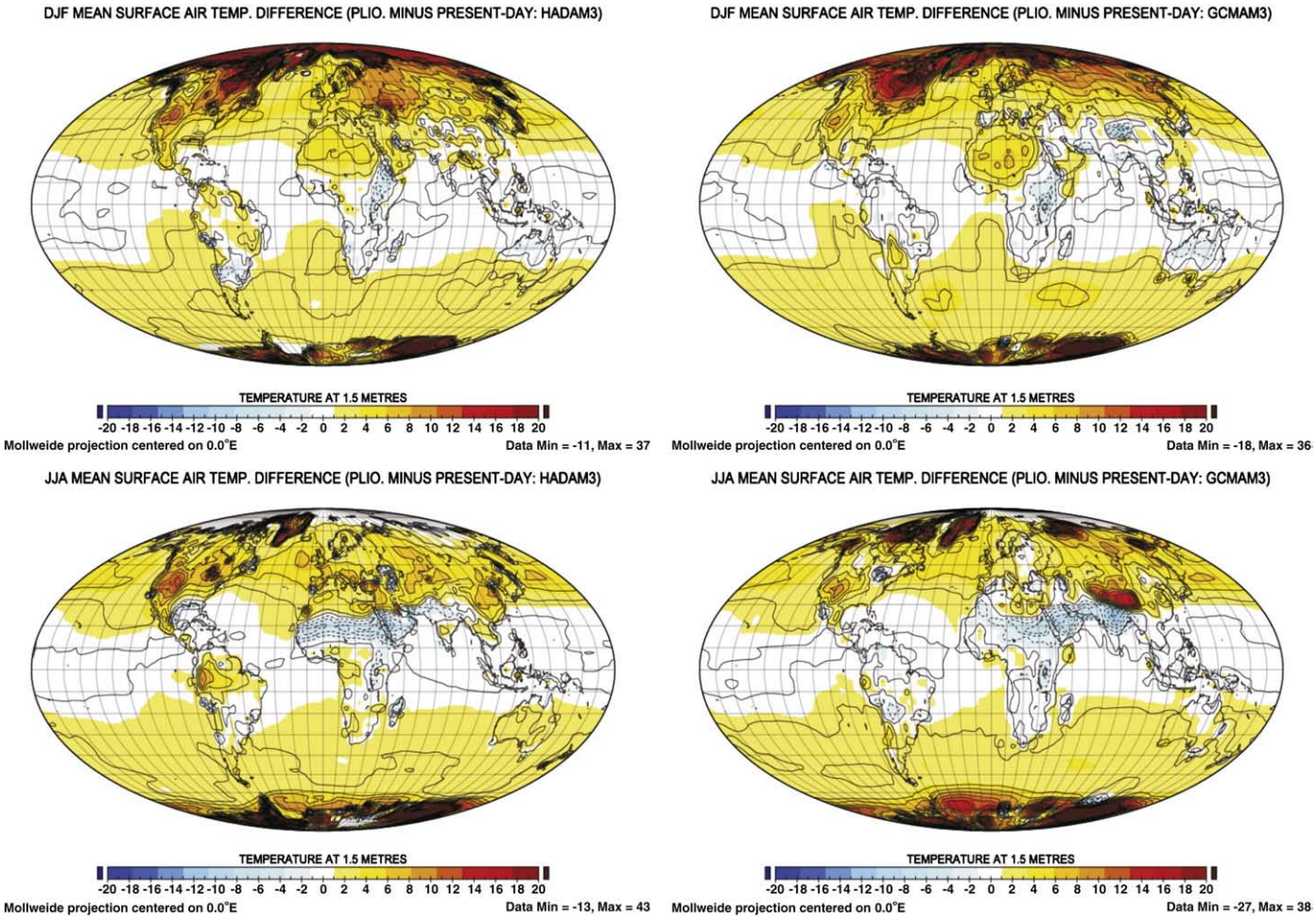

Fig. 2. Showing mean differences in December, January and February (DJF) and June, July and August (JJA) surface air temperatures (°C) for the mid-Pliocene and present-day predicted by the HadAM3 and GCMAM3 climate models. Modern coastlines shown.

this region. Modest increases (5 to 10%) are predicted by both models over Australia. Both models reduce total cloud cover over the North Atlantic, although this is most pronounced in HadAM3. Cloud cover over central and southern parts of North America is reduced by 5 to 20% in HadAM3, a trend not replicated by GCMAM3. The increase in Arctic cloud cover in HadAM3 is restricted to the DJF season (Fig. 4). The reduction over the North Atlantic and United States of America in HadAM3 is most pronounced during JJA. Increases over North Africa in both models occur during JJA (Fig. 4).

The increase in cloud cover over Antarctica and Greenland (and in HadAM3 during December, January and February (DJF) in the Arctic as a whole) is a result of reduced land and sea ice and the greater extent of relatively warm and open water in the mid-Pliocene experiments (specified from the PRISM2 data set). This in turn results in greater evaporation taking place in these regions. This relationship was also detected in the mid-Pliocene simulation using the NCAR GENESIS GCM (Sloan et al., 1996) and has been discussed by Ramanathan et al. (1989), Raymo et al. (1990), Covey et al. (1991) and Sloan and Rea (1995). Cloud cover at high-latitudes generally acts to warm climate. Both mid-Pliocene model simulations suggest that clouds are acting as a positive feedback mechanism to the high-latitude warming although this is most clearly expressed in HadAM3. In the tropics the dominant changes in precipitation coincide with the strengthened summer monsoons of Africa and India, and in areas that experience changed precipitation during both DJF and JJA. The large increases in cloud cover over Africa appear to be responsible for much of the surface air temperature decrease in that region.

4. Mid-Pliocene — GCMAM3 minus HadAM3

4.1. Surface air temperature (°C)

Differences in annual zonal mean surface air temperatures over land indicate that the GCMAM3 is ~1 °C cooler than HadAM3 between 60° north and 60° south of the equator (Fig. 1). North of 70° GCMAM3 temperatures become progressively cooler than HadAM3. At the pole GCMAM3 is more than 6 °C cooler than the HadAM3. Regional temperature differences exceeding 1 °C are evident over large areas of North America and northern South America, where GCMAM3 is cooler. Across Africa and Europe GCMAM3 is also cooler than HadAM3, but it simulates a warmer climate over southern South America than HadAM3. In Asia there is a complex pattern of difference with GCMAM3 predicting cooler temperatures over China/Tibet and warmer surface temperatures than HadAM3 over India (Figs. 5 and 6).

During DJF, the difference between GCMAM3 and HadAM3 Arctic temperatures increase to more than 16 °C (Figs. 5 and 6). In the Southern Hemisphere, GCMAM3 temperatures diverge from HadAM3 from 70° south towards the pole. Regionally, the GCMAM3 predicts warmer temperatures than HadAM3 over large areas of northern North America (Figs. 5 and 6) and across the Gulf coast states. Over South America a very similar pattern of difference to that described for the annual mean is seen with GCMAM3 cooler across Brazil and most other northern countries, whereas it is warmer than HadAM3 in the south over the Andes and Argentina. GCMAM3 predicts warmer temperatures than HadAM3 over North Africa and cooler temperatures in

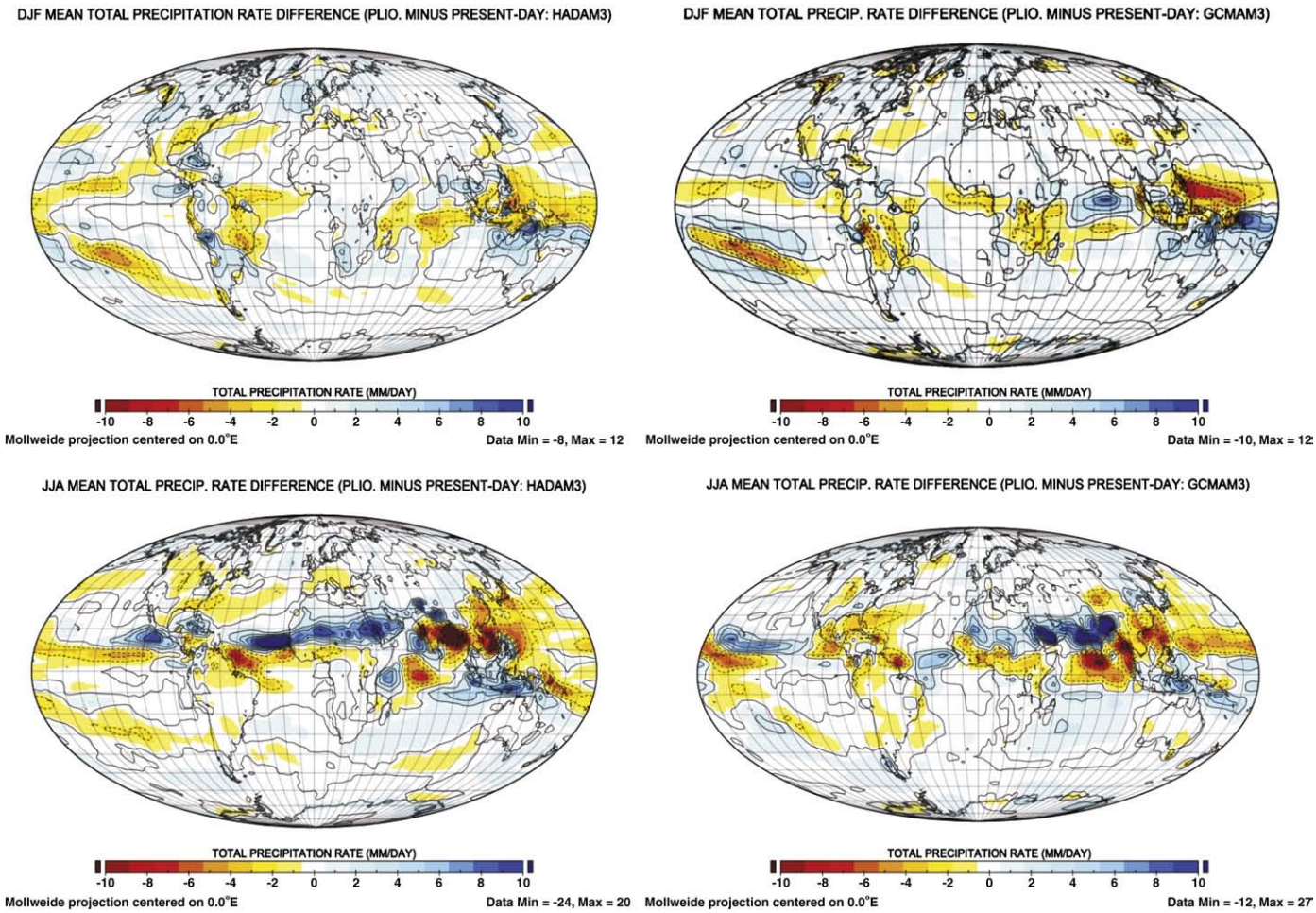

Fig. 3. Showing mean differences in December, January and February (DJF) and June, July and August (JJA) total precipitation rate (mm/day) for the mid-Pliocene and present-day predicted by the HadAM3 and GCMAM3 climate models. Modern coastlines shown.

parts of central and southern Africa. Northern Asia is substantially warmer in GCMAM3 than HadAM3, similar to the situation over Canada, and there are more regionally confined differences across western China and India where, again, the GCMAM3 is warmer.

During JJA the ~1 °C difference between the GCMAM3 and HadAM3 models is apparent equatorward of 60° in both hemispheres. This discrepancy increases to 2 °C in the Arctic (Figs. 5 and 6), and over Antarctica GCMAM3 is warmer than HadAM3. Regionally, GCMAM3 predicts temperatures that are lower than HadAM3, with the exception of parts of southern South America, Western Australia and sporadically throughout Africa and Asia (Figs. 5 and 6).

4.2. Total precipitation rate (mm/day)

As an annual mean, GCMAM3 generally has a reduced precipitation rate compared to HadAM3 in the extra-tropics (Figs. 1, 5 and 6), in line with the generally cooler surface air temperatures predicted by this model. The largest differences between the models are noted in the tropics and mid-latitudes. Differences in the position of the ITCZ are evident at nearly all longitudes, though it is generally shifted northward in the GCMAM3. This is consistent with the increased Northern Hemisphere equator-to-pole temperature gradient in GCMAM3, which is a result of its significantly cooler temperatures in the Arctic compared to HadAM3. In the eastern equatorial Pacific, GCMAM3 precipitation rates are lower (by a maximum of 4 mm/day) than those of HadAM3 (Figs. 5 and 6). In mid-latitudes GCMAM3 predicts lower precipitation rates than HadAM3, expressed most clearly in the Northern Hemisphere during winter (Figs. 5 and 6) especially along the North Atlantic Gulf Stream storm track and across the Icelandic Low.

The seasonal response of precipitation rates in monsoon regions is complex. However, GCMAM3 predicts higher precipitation rates in Northwest Africa during JJA. The zone of maximum precipitation over India, Tibet and China is shifted further to the East in GCMAM3, a result seen during JJA but most clearly demonstrated in the annual mean. GCMAM3 precipitation rate over the Indian Ocean is also significantly lower than HadAM3 in both winter and summer (Figs. 5 and 6).

4.3. Total cloud cover (%) — anomaly minus anomaly

Subtracting GCMAM3 total cloud cover anomalies (mid-Pliocene minus present-day) from cloud cover anomalies predicted by HadAM3 indicates that GCMAM3 is less sensitive to changes in high-latitude and polar cloud cover than HadAM3 (Fig. 7). This is seen in the annual mean but most clearly during DJF in the Arctic. Conversely, GCMAM3 is more sensitive than HadAM3 over most of North America (Fig. 7). GCMAM3 simulates an increase in total cloud cover over low to mid-latitude ocean regions which is not, in the main, reproduced by HadAM3. HadAM3 predicts a greater degree of cloud cover increase over North Africa and Australia during JJA compared to GCMAM3. These major trends mirror many of the differences in mid-Pliocene surface air temperatures seen between the two models in Figs. 5 and 6.

5. Discussion

5.1. GCMAM3 and HadAM3 compared

In this section we focus on, and offer potential reasons to explain, the three largest differences in mid-Pliocene climate between the GCMAM3 and HadAM3 models.

5.1.1. Arctic Ocean, Siberian, and northern North American surface air temperatures

The surface air temperature discrepancy between the two models in the Arctic and surrounding continental regions is perhaps the single most obvious difference between the two mid-Pliocene simulations. Temperature differences in winter exceed 15 °C over a region with prescribed sea ice and SSTs, which is astonishing. The fact that the peak anomaly occurs during winter in regions poleward of the Arctic Circle, where no sunlight is incident, rules out any sea ice or snow albedo effects as the likely cause of the differing temperatures. Parameterized minimum leads fraction differs by as much as 5% between the two GCMs, thus accounting for increased heat and moisture transfer from the Arctic Ocean to the atmosphere in HadAM3, an effect that may actually become predominant during winter months. GCMAM3 uses lead fractions for specified sea ice regions based entirely on the fractional area of ice designated in the climatological input files. In several Arctic grid cells, the PRISM2 winter sea ice boundary conditions include 100% ice cover (i.e. no leads fraction). A sensitivity test conducted with GCMAM3 shows that if a minimum leads fraction of 6% is incorporated into the model's sea ice parameterization, surface air temperatures over the pole could be warmed as much as 13 °C, although the effect was much less (<3 °C) at most sea ice locations. Similarly, tests using HadAM3 that examined the effects of 0% vs. 10% lead fraction (Haywood, 2001) resulted in temperature decreases of 5 °C–7 °C. Considering the opposite impacts in the two GCM sensitivity tests, and given that the models routinely use techniques for lead inclusion that differ, we believe that this, associated with differences in winter total cloud cover between the models (Figs. 4 and 7), account for much of the high-latitude temperature difference in the mid-Pliocene simulations. It should be noted that both GCMAM3 and HadAM3 perform best in their respective control runs using different values for sea ice lead fractions, so changing the minimum leads is not something that would necessarily improve the overall simulation capability of either GCM, and may, in fact, degrade the control runs if tried. Future GCM intercomparisons might avoid this issue by incorporating a minimum leads fraction into the PRISM2 sea ice inputs (or other palaeoclimate inputs) using some agreed upon algorithmic modification.

5.1.2. Mid-latitude precipitation rates

GCMAM3 predicts lower precipitation rates than HadAM3 in the mid-latitudes. This is expressed most clearly in the Northern Hemisphere during winter (DJF; see Figs. 5 and 6). One potential reason for this difference is that HadAM3 has greater horizontal resolution than GCMAM3, which could be influencing the cyclogenesis and subsequent intensification of mid-latitude storms, as well as other

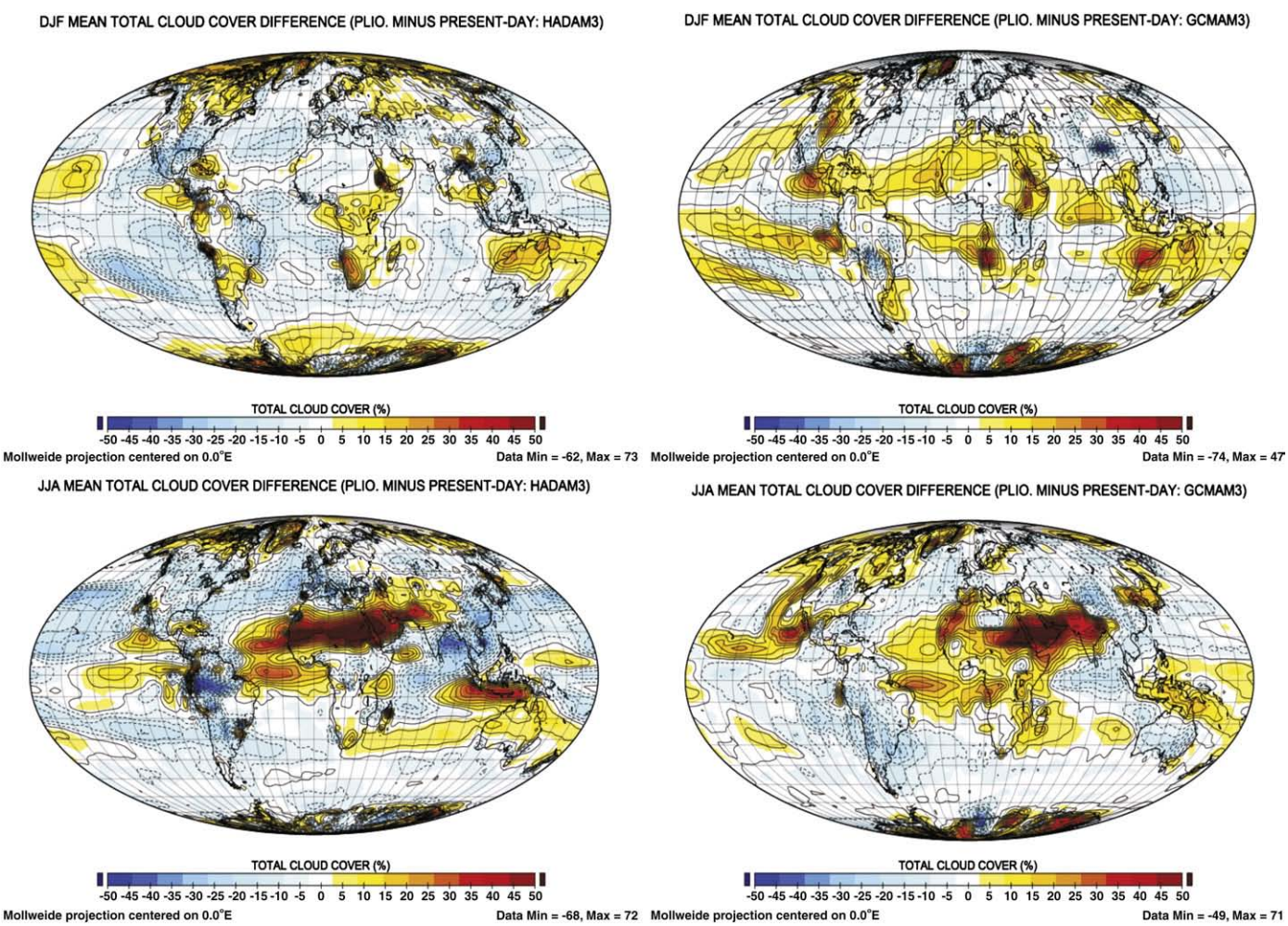

Fig. 4. Showing mean differences in December, January and February (DJF) and June, July and August (JJA) total cloud cover (%) for the mid-Pliocene and present-day predicted by the HadAM3 and GCMAM3 climate models. Modern coastlines shown.

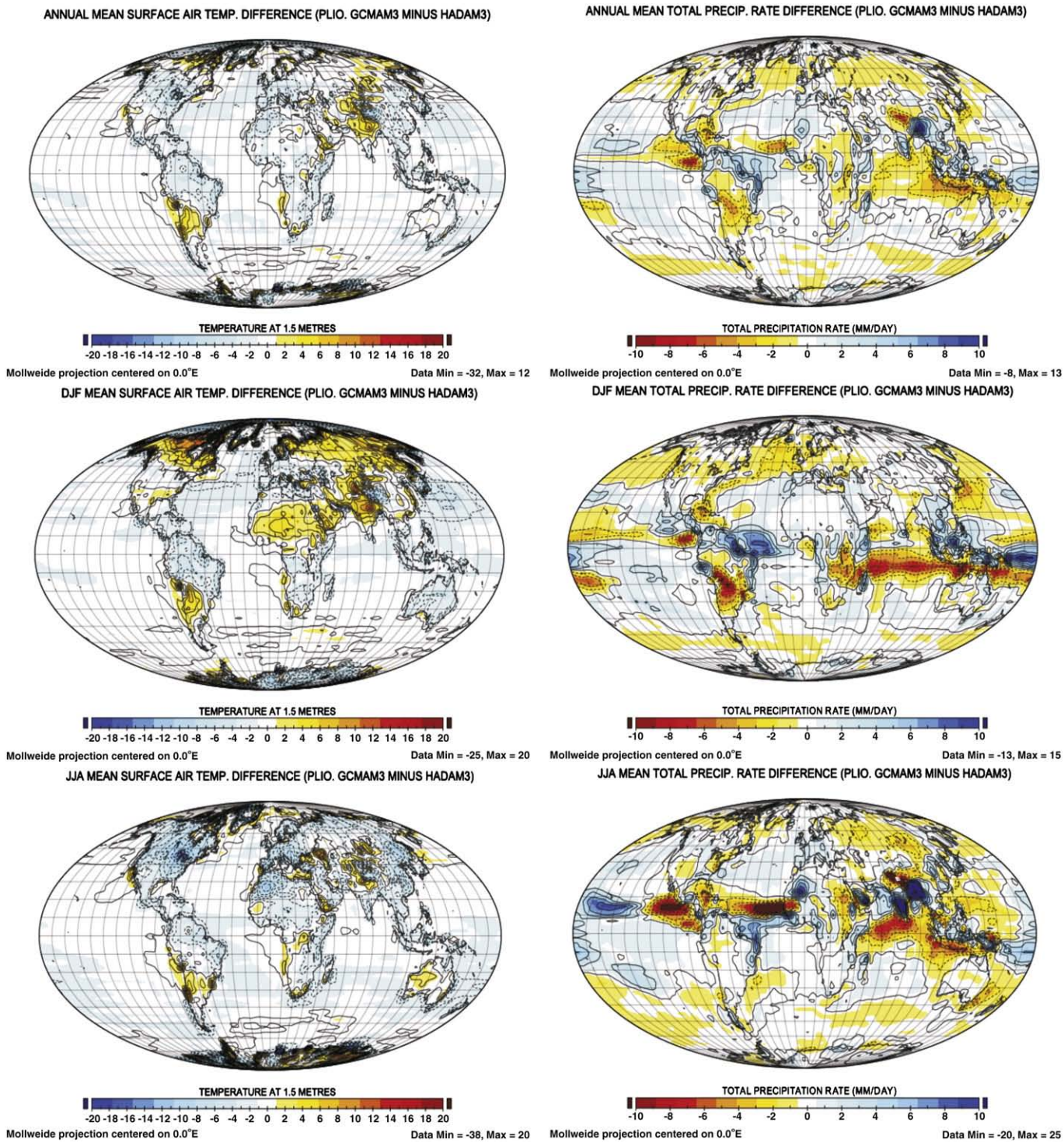

Fig. 5. Showing differences in mid-Pliocene annual mean, December, January and February (DJF) and June, July and August (JJA), surface air temperatures (°C) and total precipitation rate (mm/day) between the GCMAM3 and HadAM3 climate models. Modern coastlines shown.

important processes involved in the generation of convective and large-scale precipitation. However, the impact of increasing resolution on precipitation is not direct and very complex in numerical climate models (Pope et al., 2001). The GCMAM3 as explained above uses a quadratic upstream scheme for moisture advection that effectively increases resolution of the model's horizontal grid to better than $2° \times 2°$, and increases moisture convergence correspondingly (Schmidt et al., 2006; Rind et al., 2007).

A significant effort has been made to examine the impact of increasing horizontal, as well as vertical, resolution on precipitation amount, type and geographical distribution. In the case of HadAM3, Pope and Stratton (2002) found that at mid-latitudes, changes in precipitation that occurred through increasing horizontal resolution from N48 ($2.5° \times 3.75°$) to N144 ($0.833° \times 1.25°$) were dominated by the shifting patterns of convection and large-scale precipitation. This demonstrated that an increase in the resolved transient vertical velocities was consistent with increased vertical transport of moisture. There was correspondingly more condensation of water vapour and less evaporation of precipitation producing more large-scale precipitation. However, less convective precipitation was seen to offset

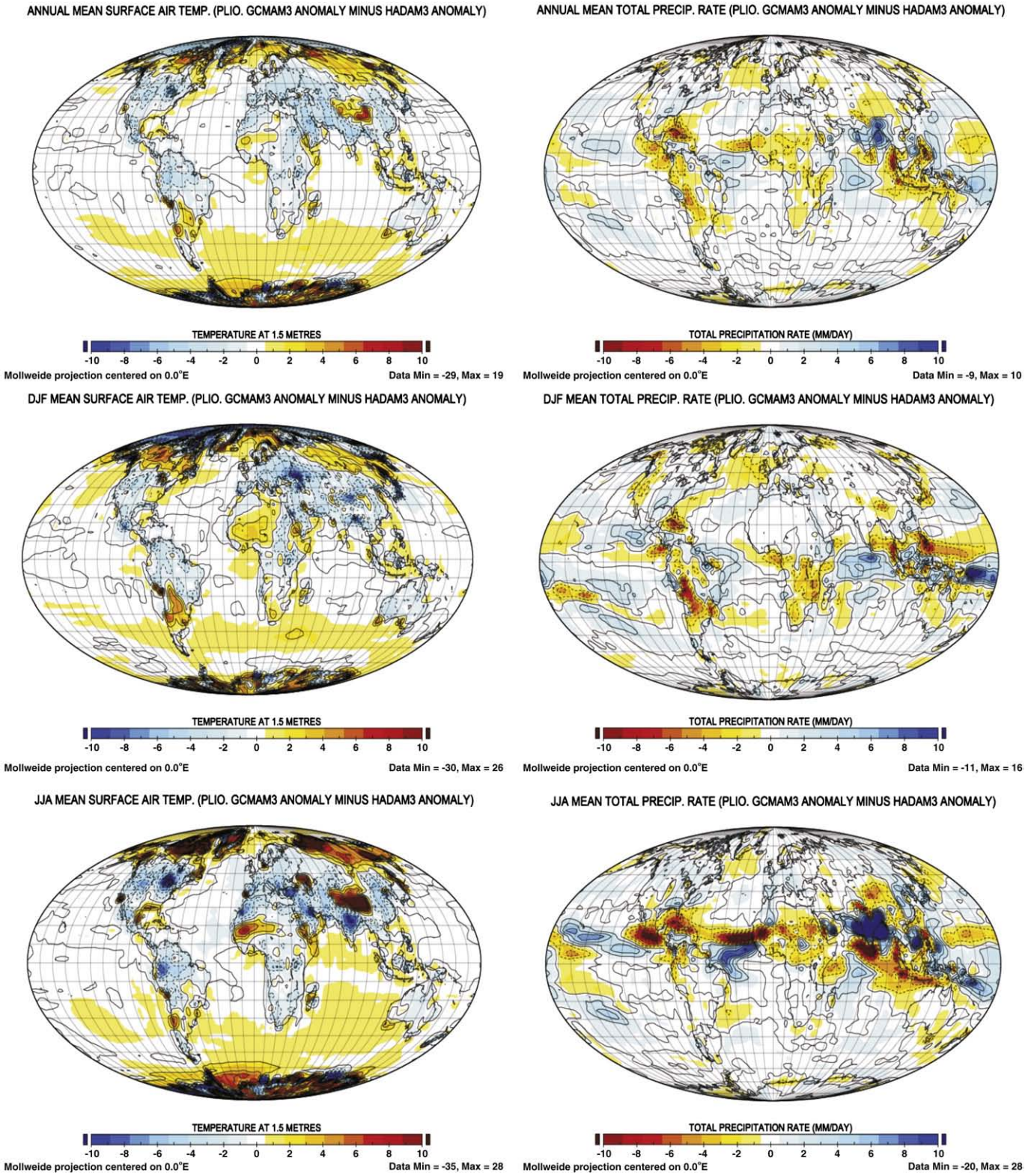

Fig. 6. Showing differences in mid-Pliocene anomalies (GCMAM3 mid-Pliocene minus GCMAM3 preset-day minus HadAM3 mid-Pliocene minus HadAM3 present-day) annual mean, December, January and February (DJF) and June, July and August (JJA), surface air temperatures (°C) and total precipitation rate (mm/day). Modern coastlines shown.

increases in large-scale precipitation at least locally and the net effect was highly dependent on location. Over the oceans, and particularly near the beginning of the storm tracks, the response was dominated by the increased large-scale precipitation. Over land and near the end of the storm tracks, the response was seen to be dominated by the decreased convective precipitation (Pope and Stratton, 2002).

Horizontal resolution also plays an important part in how well orography is represented in climate models. Pope and Stratton (2002) found that enhanced horizontal resolution led to changes in precipitation close to orography, which were similar to those described by Giorgi and Marinucci (1996) in a regional climate modelling study. However, they also found changes on a larger scale due to adjustments in the large-scale

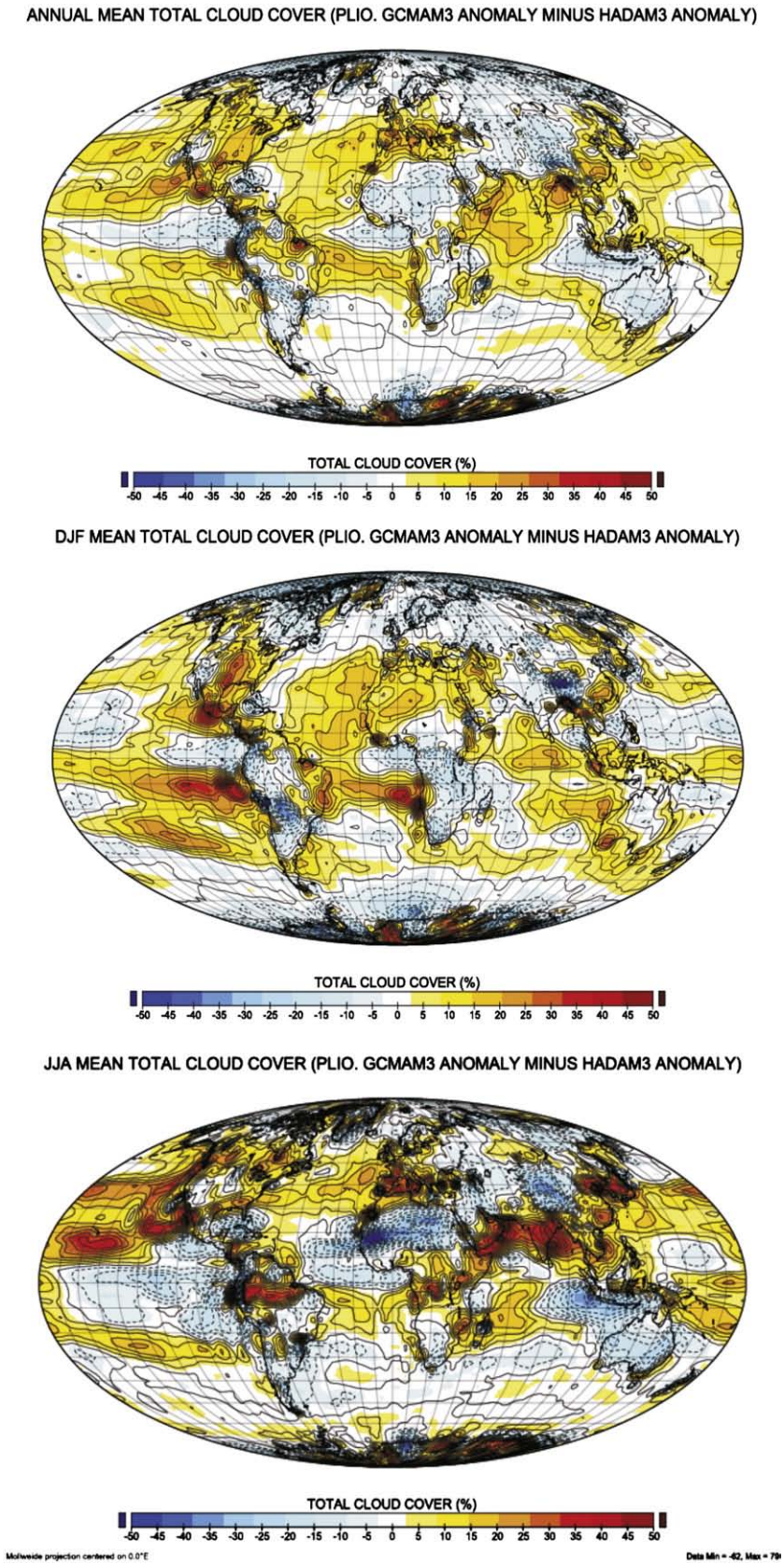

Fig. 7. Showing differences in mid-Pliocene anomalies (GCMAM3 mid-Pliocene minus GCMAM3 preset-day minus HadAM3 mid-Pliocene minus HadAM3 present-day) annual mean, December, January and February (DJF) and June, July and August (JJA), total cloud cover (%). Modern coastlines shown.

circulation, in particular off the Atlantic coast of Europe which cannot be captured in a regional model forced with boundary conditions from a low-resolution global model (Pope and Stratton, 2002).

The main regions of genesis for extra-tropical weather systems have been diagnosed within HadAM3 (Slingo et al., 2003). The results show the importance of the Rocky Mountains as the genesis region for

weather systems, as well as the cyclogenesis in the lee of the Alps over the Mediterranean. HadAM3 shows considerable skill in capturing the main regions of cyclogenesis, although the results identified reduced levels along the eastern edge of the Rocky Mountains. The regions of secondary cyclogenesis over the oceans are also well captured by HadAM3 (Slingo et al., 2003).

Given the importance of the Rocky Mountains in generating weather systems, it is worthwhile to consider the impact that different horizontal resolutions within GCMAM3 and HadAM3 may have to the representation of the Rocky Mountains and how this may affect cyclogenesis.

Studies experimenting with different horizontal and vertical resolution versions of HadAM3 have identified small but important differences in cyclogenesis over the Pacific Ocean, for example, when increasing horizontal resolution from N48 to N96, whilst at the same time increasing vertical resolution from 19 to 30 levels (Slingo et al., 2003). Although it is reasonable to propose that the difference in horizontal resolution between GCMAM3 and HadAM3 may impact cyclogenesis and therefore precipitation rate via the differing representation of the Rocky Mountains, the GCMs show less difference in the primary cyclogenic region over the central United States than they do over the Gulf Stream and in the North Atlantic where storm intensification via increased latent heat transfer comes into play. It may be worth noting that there is some consistency between this interpretation and the idea that latent heat transfer in the Arctic region is also suspected in model differences there as well.

Stratton (2004), referring to HadAM3H, suggested that increasing horizontal resolution does improve the ability of the model to simulate storms, leading to improvements in certain mean fields and more importantly to the variability as measured on the timescales of storm activity. In HadAM3, increasing horizontal resolution shifts the storm tracks poleward and increases their strength (Pope et al., 2000; Stratton, 2004). The shift in location is linked to the changes in tropospheric heating, which is in turn linked to more vigorous ascent and descent due to better resolution of cyclones. At higher horizontal resolution, cyclones decay on more realistic timescales whereas at lower resolution, the cyclones live longer (Stratton, 2004). There are indications that this correlation may not be straightforward. For example, a database of extra-tropical cyclones produced by the Goddard Institute for Space Studies, using the sea level pressure fields from the NCEP reanalysis as well as two differing resolutions of the GISS GCM, shows that higher resolution models have the ability to transport storms greater distances. The version of GCMAM used for this comparison also uses a 4th order momentum scheme, which also has a similar effect to increasing resolution, and allows storms to maintain themselves for longer and more realistic time periods.

Unfortunately, whilst an increase in horizontal resolution in HadAM3 does appear to reduce systematic error within the model (horizontal winds, temperatures, moisture, vertical velocities and transients including storm tracks and tropical variability all improve), the overall agreement between HadAM3 precipitation and the CPC Merged Analysis of Precipitation data set (CMAP; Xie and Arkin, 1997), with certain exceptions, appears to degrade (Pope and Stratton, 2002). This does not necessarily indicate that high-resolution is inappropriate; instead it may point to sensitivities in the model parameterizations that need to be investigated further (Pope et al., 2001). Pope and Stratton (2002) point out that physical parameterizations at standard resolutions (e.g. N48) have been much more extensively tested than at any other resolution, and so over a period of years, developments tend to favour this resolution. This clearly demonstrates that model parameterization must be reviewed at different horizontal resolutions. This link between resolution and physical parameterization has been identified for increasing vertical as well as horizontal resolution (increasing from 19 to 30 vertical levels) in HadAM3 (Pope et al., 2001).

Before leaving this issue, it is worthwhile to examine the overall model performance of GCMAM3 and HadAM3 for precipitation, as compared to the CMAP data set, to identify the presence of model biases which may have bearing on the model intercomparison. Pope et al. (2000) carried out an analysis of the effect of including new physical parameterization in HadAM3 compared to HadAM2b. In many geographical regions, rms (root mean square) error decreased in HadAM3 compared to HadAM2b. However, in the Northern Hemisphere extra-tropics, there is still more precipitation than the CMAP data set suggests (see Figs. 11 and 12 from Pope et al., 2000), whilst GCMAM3 predicts less precipitation than is indicated by CMAP. This suggests that the differences observed between GCMAM3 and HadAM3 could be a result of a combination of factors including horizontal resolution and also intrinsic precipitation biases in the models themselves.

5.1.3. The West African monsoon

West Africa is another region where large differences between Northern Hemisphere summer (JJA) precipitation rates are noted between the GCMAM3 and HadAM3 models for the mid-Pliocene. Seasonal variability in precipitation in this region is strongly linked to the monsoon.

The difference in West African precipitation rate for the mid-Pliocene appears to be associated with how the respective model predicts the northward migration of the ITCZ during JJA across West Africa. The ITCZ migrates further north in GCMAM3 than it does in HadAM3. Pope et al. (2000) identified increased rms errors in precipitation over Africa/India (10%) in HadAM3 compared to HadAM2b. The change over the Africa/India region arises from degradations in the monsoon circulation (Martin and Soman, 1999). There is also a tendency for the seasonal shifts in African and Asian tropical rainfall to occur earlier and be more marked in HadAM3, leading to increased rms errors in September to November and March to May (Pope et al., 2000). This aside, HadAM3 still predicts too much precipitation in West Africa associated with the summer monsoon compared to observations (ERA40 data set, not shown) and the wet bias is even greater in GCMAM3 than in HadAM3. Yet overall, BIOME 4 predicts a more realistic distribution of tropical mid-Pliocene biomes when forced with GCMAM3 climatologies, rather than those derived from HadAM3 (see next section and Table 4). So, whilst the additional sensitivity of the seasonal shift of the ITCZ in GCMAM3 apparently degrades the simulation of modern tropical precipitation (in West Africa for example) it is one ingredient which appears to actually improve the models Kappa score for the mid-Pliocene in the tropics (degree of commonality with tropical mid-terrestrial proxy data; see Section 5.2).

5.2. Data-model biome comparisons

Our data-model comparison is restricted to the terrestrial environment and is facilitated by the use of the BIOME 4 mechanistic model of

Table 4
Kappa degree of agreement for mega-biomes (and biomes) produced by mid-Pliocene BIOME 4 simulations driven by HadAM3 and GCMAM3 climatologies and also between palaeobotanical data from 202 sites. Degree of agreement between HadAM3 and GCMAM3 predictions is also shown. Location of palaeo-sites and grouping of mega-biomes are shown in Fig. 8.

Region	HadAM3 vs. GCMAM3[a]	GCMAM3 vs. palaeobotanical data[a]	HadAM3 vs. palaeobotanical data[a]
Global	0.44 (0.34)	0.33 (0.25)	0.39 (0.30)
Polar and boreal (>60° N)	0.32 (0.17)	0.23 (0.19)	0.39 (0.25)
Temperate (23.5°–60° N/S)	0.41 (0.26)	0.22 (0.17)	0.30 (0.22)
Tropical (<23.5° N/S)	0.40 (0.40)	0.38 (0.30)	0.26 (0.27)

[a] Numbers in brackets indicate agreement between biomes.

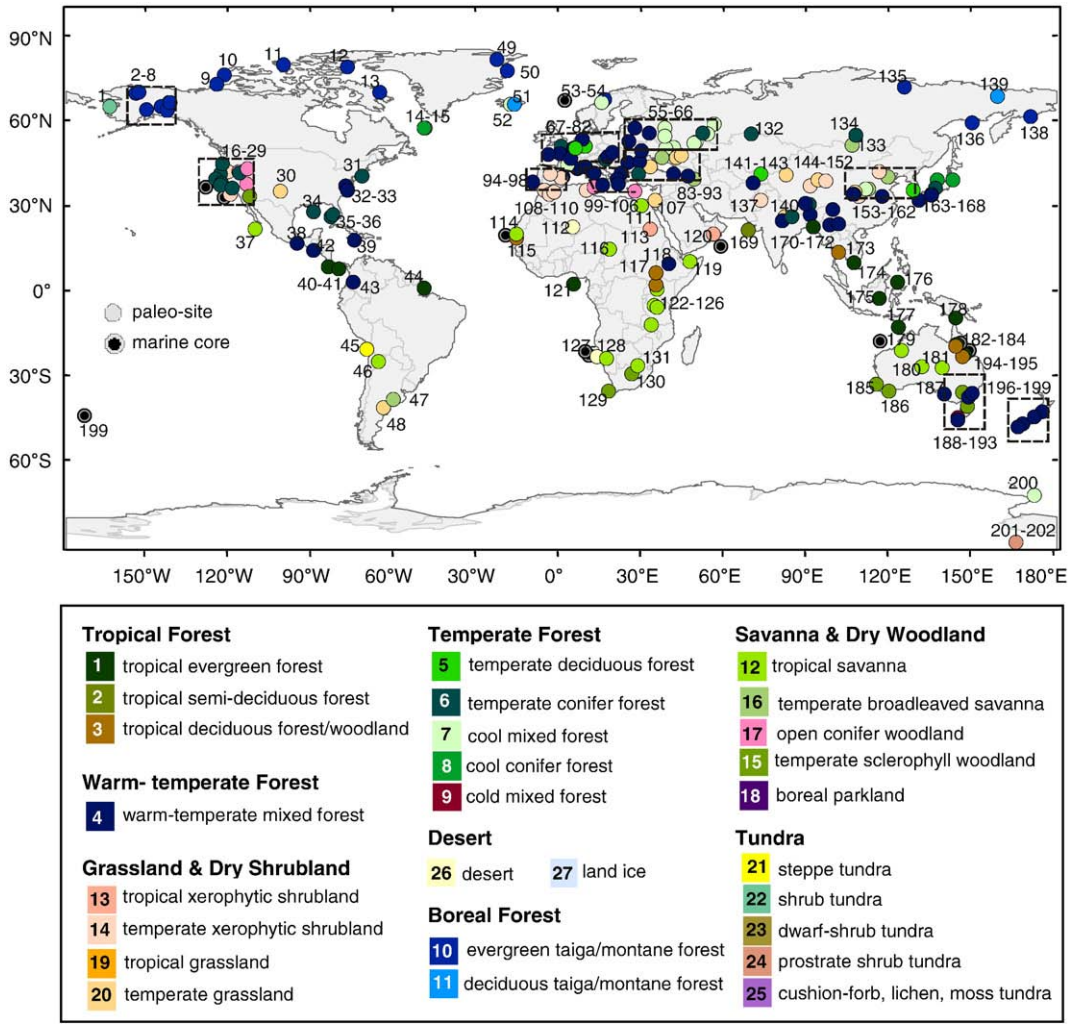

Fig. 8. Piacenzian Stage palaeobotanical sites and biomes used for the data-model comparison (for full references to palaeo-sites see Salzmann et al., 2008). Biomes were grouped in mega-biomes categories (in bold) modified after Harrison and Prentice (2003). Modern coastlines shown.

vegetation (Kaplan, 2001) to obtain results from both models for comparison with the published Pliocene biome data set. To facilitate the comparison, monthly mean surface temperature, precipitation and cloud cover from both models was used to drive BIOME 4, to provide predictions of equilibrium biome distributions to climate. We ran BIOME 4 in anomaly mode, a method often utilised in palaeoclimate modelling studies (e.g. Haxeltine and Prentice, 1996; Texier et al., 1997; Salzmann et al., 2008). The vegetation model is driven by the GCM mid-Pliocene climate, corrected by a term which accounts for biases in GCM modern climate relative to standard observations (Leemans and Cramer, 1991). Due to limited observational data for the Antarctic continent, prediction of mid-Pliocene biomes in this region was not possible. Model-predicted biomes were then compared to a state-of-the-art global reconstruction of biomes, derived from 202 localities, for the Piacenzian Stage (2.6 to 3.6 Ma as defined by Castradori et al., 1998, which encompasses the mid-Pliocene interval as defined by the PRISM project; see Dowsett et al., 1999). The Salzmann et al. (2008) data set uses the same biome classification specified in the BIOME 4 model (Fig. 8). The global data-based reconstruction of Piacenzian Stage biomes is presented in Salzmann et al. (2008), in which full details of techniques used in this form of data-model comparison are presented.

We compared our mid-Pliocene biome simulations numerically using the ArcView3.x extension for Kappa statistics (Jenness and Wynne, 2005). The Kappa statistic provides a quantitative assessment of model skill for the mid-Pliocene by measuring the degree of agreement between predicted and observed categorisations of a data set or map, whilst correcting for agreement that occurs by chance (Cohen, 1960). Kappa values (κ) between 0 and 1 are assigned a subjective label, whereby "0" means that the agreement is no better than would be expected by chance and "1" equates to a perfect match. Kappa statistics strongly depend on the number of data points and different classes selected. To avoid the minimum number of sample points per category becoming too low for meaningful Kappa statistics, we focus on the comparison of mega-biomes for which the 28 biomes were grouped into eight classes (after Harrison and Prentice, 2003).

The global biome distributions simulated by GCMAM3 and HadAM3 both indicate a mid-Pliocene climate much warmer and wetter than today (Fig. 9). Broad scale patterns of global mid-Pliocene biome distribution, which are consistent from model to model and in agreement with palaeobotanical data (Fig. 8), include:

(1) A northward shift of evergreen taiga with much reduced tundra suggested by 10–15 °C higher temperatures in the polar regions than today.
(2) A parallel northward expansion of temperate forests and grasslands in Eurasia and North America replacing boreal forests.
(3) A spread of highly diverse subtropical and warm-temperate forests with East Asian and North American affinities in middle and eastern Europe.

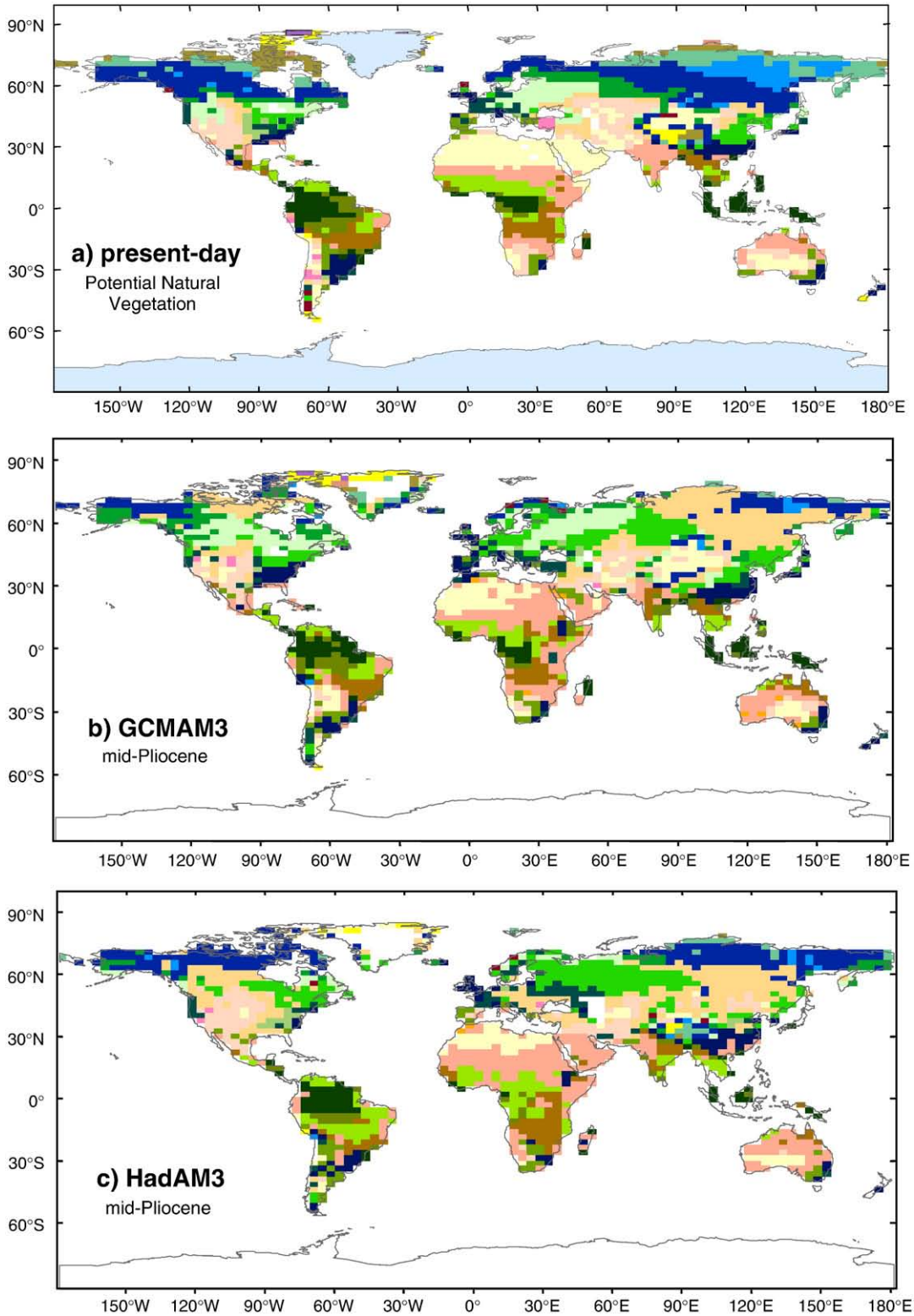

Fig. 9. a) Present-day biomes simulated by BIOME 4 using the boundary condition for PMIP1 simulations with present-day sea surface temperatures and a CO_2 concentration of 324 ppmv (Bonfils et al., 1998) and mid-Pliocene BIOME 4 simulations driven by b) GCMAM3 and c) HadAM3. BIOME 4 legend provided in Fig. 8; modern coastlines shown.

(4) An expansion of tropical savannas and woodland in Africa and Australia at the expense of deserts.

The Kappa statistic indicates that BIOME 4 predictions utilising mid-Pliocene climatologies from HadAM3 produce a slightly enhanced fit to proxy data, as compared with GCMAM3 (Table 4). However, the Kappa values reveal large regional differences. For the polar and subpolar regions, HadAM3 reproduces in agreement with palaeobotanical data a northward-displaced boreal forest zone, whereas GCMAM3 simulates for many of these regions (e.g. Siberia,

Canada) an expansion of grasslands, which is perhaps suggestive of a mid-Pliocene summer climate too dry and cold for tree growth. For the temperate zone, Kappa statistics again favour HadAM3.

However, regional inconsistencies between data-reconstructed and model-simulated biomes exist for both models. Dry grasslands predominate for the west coast of North America, and warm temperate forests for the southern Mediterranean, which mismatch the reconstruction from palaeobotanical data indicating a GCMAM3 climate simulation for the mid-Pliocene which could be dry/warm or too humid (Figs. 8 and 9). The mid-Pliocene vegetation simulated by HadAM3 differs from those of GCMAM3 by showing a predominance of grasslands in central/southeastern Europe and southern North America, both implying a regional climate possibly too warm and dry. The trend for HadAM3 to simulate a consistently lower precipitation to evaporation ratio can also be seen for most regions of the tropical vegetation zone, for which Kappa statistics indicate that BIOME 4 predictions generated using GCMAM3 climatologies provide an enhanced fit to proxy data. HadAM3 forced biome simulations that are inconsistent with palaeobotanical data and fail to reproduce the wetter tropical climates of the mid-Pliocene are particularly abundant in tropical Africa and Australia.

Our data-model comparison has identified key regions such as Canada and Siberia for which simulated vegetation changes are in the same direction. However, there are other regions and vegetation zones for which almost no agreement with palaeobotanical data is seen, and where there is little consistency between the BIOME 4 predictions produced by the GCMAM3 and HadAM3 models. These regions are particularly abundant in the temperate zone. However, overall low Kappa values for the model intercomparison (HadAM3 versus GCMAM3, Table 4) demonstrate that similar inconsistencies do also occur for other climate zones.

For HadAM3, several data-model mismatches can be clearly related to the prescription of static vegetation in our data-model comparison. Previous studies have demonstrated that mid-Pliocene simulations compare most favourably to palaeo-data when vegetation–climate feedbacks are included (Haywood and Valdes, 2006). The implementation of a dynamic vegetation model (TRIFFID: Top-down Representation of Interactive Flora and Foliage Including Dynamics) in HadAM3 increases precipitation in tropical regions and therefore resolves the described problems of HadAM3 to correctly simulate mid-Pliocene biomes for tropical Africa, central/southeastern Europe and southern North America (Haywood and Valdes, 2006; Salzmann et al., 2008).

5.3. Future direction

This study is an initial contribution to the new Pliocene Climate Modelling Intercomparison Project (Plio-MIP) being undertaken as part of the PRISM Project and PMIP2. Future studies will include results from other atmospheric General Circulation Models as well as comparisons derived from fully coupled ocean–atmosphere GCMs which will facilitate a broader data-model comparison including the enormous volume of multi-proxy SST estimates now available for the mid-Pliocene (e.g. Dowsett et al., 1996; Dowsett, 2007b). The study has highlighted the potential importance of model resolution in controlling a number of well documented mid-Pliocene climate characteristics (e.g. the degree of precipitation increase in storm tracks); although, it will be important to use versions of models where the parameterizations are developed for, and appropriate to, a given resolution. This provides a strong justification for applying the latest cutting-edge generation of atmospheric models to the simulation of mid-Pliocene climate and to continue the iterative process of improving both data interpretation and model examination for this critical period of global warming.

6. Conclusions

In this paper we present the initial results from a comparison of mid-Pliocene surface air temperature and precipitation estimates generated by the Goddard Institute for Space Studies (GISS) Global Climate Middle Atmosphere Model (GCMAM3) and the Hadley Centre for Climate Prediction and Research atmospheric-GCM (HadAM3). This is a first attempt to assess the degree of model-dependency of existing climate predictions for this interval.

(1) Overall both models reproduce and are consistent in the prediction of the large scale changes in surface air temperatures and precipitation between the mid-Pliocene and present-day. However, significant differences are noted in detail on local and regional scales. The regions where the models show most divergence include the Arctic (surface air temperatures especially during the winter), the mid-latitudes (total precipitation rate especially during the winter) and in regions influenced by the summer monsoon (temperature and precipitation).

(2) Potential reasons for these differences include the specification of sea ice leads fraction within the models and how leads are represented in the models (actual representation within the model code or via alteration of the pre-processed sea ice boundary conditions files used by the models), numerical instabilities commonly encountered at the high-latitudes due to the convergence of model grid boxes, the different horizontal resolution of the two models which may influence vertical motion within the atmosphere and hence large-scale precipitation as well as the representation of orography.

(3) GCM climatologies are used to drive the BIOME 4 mechanistic model of vegetation, and these predictions are compared with an extant data set of data reconstructed Pliocene biomes. Statistical analysis suggests that HadAM3 predictions are more consistent with palaeo-data in mid-to-high-latitudes, whereas GCMAM3 predictions in the tropics provide an enhanced fit to proxy data, compared with HadAM3.

Acknowledgements

The authors would like to acknowledge the National Science Foundation (US) and the Natural Environment Research Council (UK) for financial support. This work is product of the PRISM Project and the NERC funded British Antarctic Survey core programme GEACEP (Greenhouse to Ice-house Evolution of the Antarctic Cryosphere and Palaeoenvironment). The work was carried out under the umbrella of the Pliocene Climate Modelling Intercomparison Project (Plio-MIP) which is part of the international Palaeoclimate Modelling Intercomparison Project (PMIP).

References

Abramopoulos, F., Rosenzweig, C., Choudhury, B., 1988. Improved ground hydrology calculations for global climate models (GCMs): soil water movement and evapotranspiration. J. Climate 1, 921–941. doi:10.1175/1520-0442(1988)001<0921:IGHCFG>2.0.CO;2.

Balachandran, N.K., Rind, D., 1995. Modeling the effects of UV variability and the QBO on the troposphere/stratosphere system. Part I: the middle atmosphere. J. Climate 8, 2058–2079. doi:10.1175/1520-0442(1995)008<2058:MTEOUV>2.0.CO;2.

Barron, E.J., Washington, W.M., 1982. Cretaceous climate: a comparison of atmospheric simulations with the geologic record. Palaeogeogr. Palaeoclimatol. Palaeoecol. 40, 103–133.

Bonfils, C.J., Lewden, D., Taylor, K.E., 1998. Summary documentation of the PMIP models: main document directory. PMIP Documentation (PCMDI Report). http://www-lsce.cea.fr/pmip.

Castradori, D., Rio, D., Hilgen, F.J., Lourens, L.J., 1998. The Global Standard Stratotype-section and Point (GSSP) of the Piacenzian (Middle Pliocene). Episodes 21, 88–93.

Cattle, H., Crossley, J., 1995. Modelling Arctic climate change. Philosophical Transactions of the Royal Society of London A352, 201–213.

Chandler, M.A., Rind, D., Thompson, R.S., 1994. Joint investigations of the middle Pliocene climate II: GISS GCM Northern Hemisphere results. Glob. Planet. Change 9, 197–219. doi:10.1016/0921-8181(94)90016-7.

Cohen, J., 1960. A coefficient of agreement for nominal scales. Educ. Psychol. Meas. 2, 37–46.

Covey, C., Taylor, K.E., Dickson, R.E., 1991. Upper limit for sea ice albedo feedback contribution to global warming. J. Geophys. Res. 96, 9169–9174.

Cox, P., Betts, R., Bunton, C., Essery, R., Rowntree, P.R., Smith, J., 1999. The impact of new land-surface physics on the GCM simulation and climate sensitivity. Clim. Dyn. 15, 183–203.

Cronin, T.M., Dowsett, H.J., 1990. A quantitative micropaleontologic method for shallow marine paleoclimatology: application to Pliocene deposits of the western North Atlantic Ocean. Mar. Micropaleontol. 16 (1/2), 117–148.
Cusack, S., Slingo, A., Edwards, J.M., Wild, M., 1998. The radiative impact of a simple aerosol climatology on the Hadley Centre GCM. Q. J. R. Meteorol. Soc. 124, 2517–2526.
Cusack, S., Edward, J.M., Wild, M., 1999. Investigating K-distribution methods for parametrizing gaseous absorption in the Hadley Centre climate model. J. Geophys. Res. 104, 2051–2057.
DeConto, R.M., Pollard, D., 2003. Rapid Cenozoic glaciation of Antarctica induced by declining atmospheric CO_2. Nature 421, 245–249.
Del Genio, A.D., Yao, M.-S., Kovari, W., Lo, K.K.-W., 1996. A prognostic cloud water parameterization for global climate models. J. Climate 9, 270–304. doi:10.1175/1520-0442(1996)009<0270:APCWPF>2.0.CO;2.
Dowsett, H.J., 2007a. The PRISM palaeoclimate reconstruction and Pliocene sea-surface temperatures. In: Williams, M., Haywood, A.M., Gregory, J., Schmidt, D. (Eds.), Deep-time Perspectives on Climate Change: Marrying the Signal From Computer Models and Biological Proxies. . The Micropalaeontological Society, Special Publication. Geol. Soc., London, pp. 459–480.
Dowsett, H.J., 2007b. Faunal re-evaluation of mid-Pliocene conditions in the western equatorial Pacific. Micropaleontology 53, 447–456.
Dowsett, H., Barron, J., Poore, R., 1996. Middle Pliocene sea surface temperatures: a global reconstruction. Mar. Micropaleontol. 27, 13–26.
Dowsett, H.J., Barron, J.A., Poore, R.Z., Thompson, R.S., Cronin, T.M., Ishman, S.E., Willard, D.A., 1999. Middle Pliocene paleoenvironmental reconstruction: PRISM2. USGS Open File Report, pp. 99–535. http://pubs.usgs.gov/openfile/of99-535.
Edwards, J.M., Slingo, A., 1996. Studies with a flexible new radiation code 1: choosing a configuration for a large-scale model. Q. J. R. Meteorol. Soc. 122, 689–719.
Giorgi, F., Marinucci, M.R., 1996. An investigation of the sensitivity of the simulated precipitation to model resolution and its implications for climate studies. Mon. Weather Rev. 124, 148–166.
Gregory, D., 1995. A consistent treatment of the evaporation of rain and snow for use in large-scale models. Mon. Weather Rev. 123, 2716–2732.
Gregory, D., Rowntree, P.R., 1990. A mass flux convection scheme with representation of cloud ensemble characteristics and stability dependent closure. Mon. Weather Rev. 118, 1483–1506.
Gregory, D., Morris, D., 1996. The sensitivity of climate simulations to the specification of mixed phase clouds. Clim. Dyn. 12, 641–651.
Gregory, D., Shutts, G.L., Mitchell, J.R., 1998. A new gravity-wave-drag scheme incorporating anisotropic orography and low-level wave breaking: impact upon climate of the UK Meteorological Office Unified Model. Q. J. R. Meteorol. Soc. 124, 463–494.
Gregory, D., Kershaw, R., Inness, P.M., 1997. Parametrisation of momentum transport by convection II: tests in single column and general circulation models. Q. J. R. Meteorol. Soc. 123, 1153–1183.
Hansen, J., Russell, G., Rind, D., Stone, P., Lacis, A., Lebedeff, S., Ruedy, R., Travis, L., 1983. Efficient three-dimensional global models for climate studies: models I and II. Mon. Weather Rev. 111, 609–662.
Harrison, S.P., Prentice, I.C., 2003. Climate and CO_2 controls on global vegetation distribution at the last glacial maximum: analysis based on palaeovegetation data, biome modelling and palaeoclimate simulations. Glob. Chang. Biol. 9, 983–1004.
Haxeltine, A., Prentice, I.C., 1996. BIOME3: an equilibrium terrestrial biosphere model based on ecophysiological constrains, resource availability, and competition among plant functional types. Glob. Biogeochem. Cycles 10, 693–709.
Haywood, A.M., (2001). Evaluating GCM reliability against the Pliocene geological record. Reading University PhD thesis, Reading University, UK.
Haywood, A.M., Valdes, P.J., 2004. Modelling Pliocene warmth: contribution of atmosphere, oceans and cryosphere. Earth Planet. Sci. Lett. 218, 363–377. doi:10.1016/S0012-821X(03)00685-X.
Haywood, A.M., Valdes, P.J., 2006. Vegetation cover in a warmer world simulated using a dynamic global vegetation model for the mid-Pliocene. Palaeogeogr. Palaeoclimatol. Palaeoecol. 237, 412–427.
Haywood, A.M., Valdes, P.J., Sellwood, B.W., 2000a. Global scale palaeoclimate reconstruction of the middle Pliocene climate using the UKMO GCM: initial results. Glob. Planet. Change 25, 239–256. doi:10.1016/S0921-8181(00)00028-X.
Haywood, A.M., Sellwood, B.W., Valdes, P.J., 2000b. Regional warming: Pliocene (3 Ma) paleoclimate of Europe and the Mediterranean. Geology 28, 1063–1066. doi:10.1130/0091-7613(2000)28<1063:RWPMPO>2.0.CO;2.
Haywood, A.M., Valdes, P.J., Peck, V.L., 2007. A permanent El Niño-like state during the Pliocene? Paleoceanography 22, PA1213. doi:10.1029/2006PA001323.
Hoar, M.R., Palutikof, J.P., Thorne, M.C., 2004. Model intercomparison for the present day, the mid-Holocene, and the Last Glacial Maximum over Western Europe. J. Geophys. Res. 109 (8), D08104.
Huber, M., Caballero, R., 2003. Eocene El Niño: evidence for robust tropical dynamics in the "Hothouse". Science 299, 877–881.
IPCC, 2007. Climate change 2007: the physical science basis. In: Solomon, S., Qin, D., Manning, M., Chen, Z., Marquis, M., Averyt, K.B., Tignor, M., Miller, H.L. (Eds.), Contribution of Working Group I to the Fourth Assessment Report of the Intergovernmental Panel on Climate Change. Cambridge University Press, Cambridge, United Kingdom.
Jansen, E., Overpeck, J., Briffa, K.R., Duplessy, J.-C., Joos, F., Masson-Delmotte, V., Olago, D., Otto-Bliesner, B., Peltier, W.R., Rahmstorf, S., Ramesh, R., Raynaud, D., Rind, D., Solomina, O., Villalba, R., Zhang, D., 2007. Palaeoclimate. In: Solomon, S., Qin, D., Manning, M., Chen, Z., Marquis, M., Averyt, K.B., Tignor, M., Miller, H.L. (Eds.), Climate Change 2007: The Physical Science Basis. Contribution of Working Group I to the Fourth Assessment Report of the Intergovernmental Panel on Climate Change. Cambridge University Press, Cambridge, United Kingdom.
Jasperson, W.H., Nastrom, G.D., Fritts, D.C., 1990. Further study of terrain effects on the mesoscale spectrum of atmospheric motions. J. Atmos. Sci. 47, 979–987.
Jenness, J., Wynne, J.J., 2005. Cohen's Kappa and classification table metrics 2.0: an ArcView 3× extension for accuracy assessment of spatially explicit models. U.S. Geological Survey Open-File Report 2005-1363. U.S. Geological Survey, Southwest Biological Science Center, Flagstaff, AZ.
Jiang, D., Wang, H., Ding, Z., Lang, X., Drange, H., 2005. Modeling the middle Pliocene climate with a global atmospheric general circulation model. J. Geophys. Res. 110, D14107. doi:10.1029/2004JD005639.
Joussaume, S., Taylor, K.E., 1995. Status of the Paleoclimate Modeling Intercomparison Project (PMIP). Proceedings of the First International AMIP Scientific Conference. WCRP Report, pp. 425–430.
Kaplan, J.O., (2001). Geophysical Applications of Vegetation Modeling. Ph.D. Thesis, Lund University, Lund.
Kim, S.J., Crowley, T.J., 2000. Increased Pliocene North Atlantic deep water — cause or consequence of Pliocene warming? Paleoceanography 15, 451–455.
Kürschner, W.M., Van der Burgh, J., Visscher, H., Dilcher, D.L., 1996. Oak leaves as biosensors of late Neogene and early Pleistocene paleoatmospheric CO_2 concentrations. Mar. Micropaleontol. 27 (1/4), 299–312.
Kutzbach, J.E., Otto-Bliesner, B.L., 1982. The sensitivity of the African–Asian monsoonal climate to orbital parameter changes for 9000 yr B.P. in a low-resolution general circulation model. J. Atmos. Sci. 39, 1177–1188.
Lacis, A.A., Oinas, V., 1991. A description of the correlated k distributed method for modeling nongray gaseous absorption, thermal emission, and multiple scattering in vertically inhomogeneous atmospheres. J. Geophys. Res. 96, 9027–9063. doi:10.1029/90JD01945.
Leemans, R., Cramer, W.P., 1991. The IIASA Database for Mean Monthly Values of Temperature, Precipitation and Cloudiness on a Global Terrestrial Grid. International Institute for Applied Systems Analysis, Laxenberg, p. 62.
Martin, G.M., Soman, M.K., 1999. Effects of changing physical parametrisations on the simulation of the Asian summer monsoon in the U.K. Meteorological Office Unified Model. Hadley Centre Technical Note No. 17. Hadley Centre, The Met. Office, London Road, Bracknell, U.K.
Matthews, E., 1985. Prescription of land-surface boundary conditions in GISS GCM II: a simple method based on high-resolution vegetation data bases. NASA Report TM 86096. 20 pp.
NOAA, 1988. Data Announcement 88-MGG-02, Digital Relief of the Surface of the Earth.
Oinas, V., Lacis, A.A., Rind, D., Shindell, D.T., Hansen, J.E., 2001. Radiative cooling by stratospheric water vapor: big differences in GCM results. Geophys. Res. Lett. 28, 2791–2794. doi:10.1029/2001GL013137.
Poore, R.Z. and Sloan, L.C., (1996). Climates and climate variability of the Pliocene, (Eds.). Mar. Micropaleontol. 27 (1/4), 326 pp.
Pope, V.D., Stratton, R.A., 2002. The processes governing horizontal resolution sensitivity in a climate model. Clim. Dyn. 19, 211–236.
Pope, V.D., Gallani, M.L., Rowntree, P.R., Stratton, R.A., 2000. The impact of new physical parametrizations in the Hadley Centre climate model — HadAM3. Climate Dynamics 16, 123–146.
Pope, V.D., Pamment, J.A., Jackson, D.R., Slingo, A., 2001. The representation of water vapor and its dependence on vertical resolution in the Hadley Centre Climate Model. J. Climate 14, 3065–3085.
Prentice, I.C., Webb III, T., 1998. BIOME 6000: reconstructing global mid-Holocene vegetation patterns from palaeoecological records. J. Biogeogr. 25, 997–1005.
Ramanathan, V., Barkstrom, B.R., Harrison, E.F., 1989. Climate and the Earth's radiation budget. Physics Today 42, 22–32.
Randall, D.A., Wood, R.A., Bony, S., Colman, R., Fichefet, T., Fyfe, J., Kattsov, V., Pitman, A., Shukla, J., Srinivasan, J., Stouffer, R.J., Sumi, A., Taylor, K.E., 2007. Climate models and their evaluation. In: Solomon, S., Qin, D., Manning, M., Chen, Z., Marquis, M., Averyt, K.B., Tignor, M., Miller, H.L. (Eds.), Climate Change 2007: The Physical Science Basis. Contribution of Working Group I to the Fourth Assessment Report of the Intergovernmental Panel on Climate Change. Cambridge University Press, Cambridge, United Kingdom.
Raymo, M.E., Rau, G.H., 1992. Plio-Pleistocene Atmospheric CO_2 Levels Inferred from POM $\delta^{13}C$ at DSDP Site 607. EOS, Transactions of the American Geophysical Union, Spring Meeting, vol. 73 (Suppl.).
Raymo, M.E., Rind, D., Ruddiman, W.F., 1990. Climatic effects of reduced Arctic sea ice limits in the GISS II general circulation model. Paleoceanography 5, 367–382.
Raymo, M.E., Grant, B., Horowitz, M., Rau, G.H., 1996. Mid-Pliocene warmth: stronger greenhouse and stronger conveyor. Mar. Micropaleontol. 27 (1/4), 313–326.
Rayner, N.A., Parker, D.E., Horton, E.B., Folland, C.K., Alexander, L.V., Rowell, D.P., Kent, E.C., Kaplan, A., 2003. Global analyses of SST, sea ice and night marine air temperature since the late nineteenth century. J. Geophys. Res. 108, 4407. doi:10.1029/2002JD002670.
Reynolds, R.W., Smith, T.M., 1995. A high-resolution global sea surface temperature climatology. J. Climatol. 8, 1571–1583.
Rind, D., Chandler, M., Lonergan, P., Lerner, J., 2001a. Climate change and the middle atmosphere: 5. Paleostratosphere in cold and warm climates. J. Geophys. Res. 106, 20195–20212. doi:10.1029/2000JD900548.
Rind, D., Suozzo, R., Balachandran, N.K., Lacis, A., Russell, G., 1988. The GISS Global Climate-Middle Atmosphere Model. Part I: Model structure and climatology. J. Atmos. Sci. 45, 329–370. doi:10.1175/1520-0469(1988)045<0329:TGGCMA>2.0.CO;2.
Rind, D., Lerner, J., Shah, K., Suozzo, R., 1999. Use of on-line tracers as a diagnostic tool in general circulation model development: 2. Transport between the troposphere and stratosphere. J. Geophys. Res. 104, 9151–9167. doi:10.1029/1999JD900006.
Rind, D., Lerner, J., McLinden, C., 2001b. Changes of tracer distributions in the doubled CO_2 climate. J. Geophys. Res. 106, 28061–28079. doi:10.1029/2001JD000439.

Rind, D., Perlwitz, J., Lonergan, P., 2005. AO/NAO response to climate change: 1. Respective influences of stratospheric and tropospheric climate changes. J. Geophys. Res. 110, D12107. doi:10.1029/2004JD005103.

Rind, D., Lerner, J., Jonas, J., McLinden, C., 2007. The effects of resolution and model physics on tracer transports in the NASA Goddard Institute for Space Studies general circulation models. J. Geophys. Res. 112, D09315. doi:10.1029/2006JD007476.

Salzmann, U., Haywood, A.M., Lunt, D.J., Valdes, P.J., Hill, D.J., 2008. A new global biome reconstruction and data-model comparison for the Middle Pliocene. Global Ecol. Biogeogr. 17, 432–447. doi:10.1111/j.1466-8238.2007.00381.x.

Schmidt, G.A., Ruedy, R., Hansen, J.E., Aleinov, I., Bell, N., Bauer, M., Bauer, S., Cairns, B., Canuto, V., Cheng, Y., Del Genio, A., Faluvegi, G., Friend, A.D., Hall, T.M., Hu, Y., Kelley, M., Kiang, N.Y., Koch, D., Lacis, A.A., Lerner, J., Lo, K.K., Miller, R.L., Nazarenko, L., Oinas, V., Perlwitz, Ja., Perlwitz, Ju., Rind, D., Romanou, A., Russell, G.L., Sato, Mki., Shindell, D.T., Stone, P.H., Sun, S., Tausnev, N., Thresher, D., Yao, M.-S., 2006. Present day atmospheric simulations using GISS ModelE: comparison to in-situ, satellite and reanalysis data. J. Climate 19, 153–192. doi:10.1175/JCLI3612.1.

Senior, C., Mitchell, J.F.B., 1993. CO_2 and climate: the impact of cloud parametrization. J. Climate 6, 393–418.

Shindell, D.T., Schmidt, G.A., Mann, M.E., Rind, D., Waple, A., 2001. Solar forcing of regional climate change during the Maunder Minimum. Science 294, 2149–2152. doi:10.1126/science.1064363.

Slingo, J., Guilyardi, E., Hodges, K., Hoskins, B., Inness, P., Lawrence, D., Neale, R., Osborne, T., Spencer, H., Yang, G.-Y., 2003. How good is the Hadley Centre climate model? Research at CGAM on Identifying and Understanding Model Systematic Errors: 1999–2002. Hadley Centre Technical Note 67, p. 61.

Sloan, L.C., Rea, D.K., 1995. Atmospheric carbon dioxide and early Eocene climate: a general circulation modeling sensitivity study. Palaeogeogr. Palaeoclimatol. Palaeoecol. 119, 275–292.

Sloan, L.C., Crowley, T.J., Pollard, D., 1996. Modeling of Middle Pliocene climate with the NCAR Genesis general circulation model. Mar. Micropaleontol. 27, 51–61.

Smith, R.N.B., 1990. A scheme for predicting layer clouds and their water content in a general circulation model. Q. J. R. Meteorol. Soc. 116, 435–460.

Sohl, L.E., Chandler, M.A., 2007. Reconstructing Neoproterozoic paleoclimates using a combined data/modelling approach. In: Williams, M., Haywood, A.M., Gregory, J., Schmidt, D. (Eds.), Deep-time Perspectives on Climate Change: Marrying the Signal From Computer Models and Biological Proxies. . The Micropalaeontology Society, Special Publication. The Geological Society, London, pp. 61–80.

Stratton, R.A., 2004. Report on Aspects of Variability in High-resolution Versions of HadAM3. Hadley Centre Technical Note 53. 31.pp.

Texier, D., de Noblet, N., Harrison, S.P., Haxeltine, A., Jolly, D., Joussaume, S., Laarif, F., Prentice, I.C., Tarasov, P., 1997. Quantifying the role of biosphere–atmosphere feedbacks in climate change: coupled model simulations for 6000 years BP and comparison with paleodata for northern Eurasia and Africa. Clim. Dyn. 13, 865–882.

Thompson, R.S., Fleming, R.F., 1996. Middle Pliocene vegetation: reconstructions, paleoclimatic inferences, and boundary conditions for climatic modeling. Mar. Micropaleontol. 27 (1/4), 13–26.

Valdes, P.J., Sellwood, B.W., 1992. A palaeoclimate model for the Kimmeridgian. Palaeogeogr. Palaeoclimatol. Palaeoecol. 95, 47–72.

Williams, M., Haywood, A.M., Gregory, J., Schmidt, D. (Eds.), 2007. Deep-time Perspectives on Climate Change: Marrying the Signal from Computer Models and Biological Proxies. . The Micropalaeontology Society, Special Publication. Geol. Soc., London. 589 pp.

Wilson, M.F., Henderson-Sellers, A., 1985. A global archive of land cover and soils data for use in General Circulation Climate Models. J. Climatol. 5, 119–143.

Xie, P., Arkin, P.A., 1997. Global precipitation: a 17-year monthly analysis based upon gauge observations, satellite estimates, and numerical model outputs. Bulletin of the American Meteorological Society 78, 2539–2558.

Zheng, W., Braconnot, P., Guilyardi, E., Merkel, U., Yu, Y., 2008. ENSO at 6 ka and 21 ka from ocean–atmosphere coupled model simulations. Clim. Dyn. 30, 745–762.